

Zeitschrift: IABSE reports = Rapports AIPC = IVBH Berichte
Band: 999 (1997)

Rubrik: Advanced composites

Nutzungsbedingungen

Die ETH-Bibliothek ist die Anbieterin der digitalisierten Zeitschriften. Sie besitzt keine Urheberrechte an den Zeitschriften und ist nicht verantwortlich für deren Inhalte. Die Rechte liegen in der Regel bei den Herausgebern beziehungsweise den externen Rechteinhabern. [Siehe Rechtliche Hinweise.](#)

Conditions d'utilisation

L'ETH Library est le fournisseur des revues numérisées. Elle ne détient aucun droit d'auteur sur les revues et n'est pas responsable de leur contenu. En règle générale, les droits sont détenus par les éditeurs ou les détenteurs de droits externes. [Voir Informations légales.](#)

Terms of use

The ETH Library is the provider of the digitised journals. It does not own any copyrights to the journals and is not responsible for their content. The rights usually lie with the publishers or the external rights holders. [See Legal notice.](#)

Download PDF: 22.12.2024

ETH-Bibliothek Zürich, E-Periodica, <https://www.e-periodica.ch>

Bond Behaviour of CFRP-Laminates for the Strengthening of Concrete Members

Ferdinand S. ROSTASY

Prof. Dr.-Ing.
TU Braunschweig
Braunschweig, Germany

Ferdinand S. Rostasy born 1932, received his civil engineering degree in 1954. After several years in construction practice he returned to research and teaching. Since 1976, he is professor of structural materials at the TU Braunschweig.

Uwe NEUBAUER

Dipl.-Ing.
TU Braunschweig
Braunschweig, Germany

Uwe Neubauer, born 1963, received his civil engineering degree in 1994. Since then he works as research engineer at the Institute for Building Materials, Concrete Construction, and Fire Protection of the TU Braunschweig.

Summary

For several reasons, in plate strengthened members a reliable bond via the epoxy joint is essential for the composite action. According to the truss analogy the ends of the plates of carbon fiber reinforced plastics (CFRP-plates) have to be anchored to the concrete. Bond tests indicated, that an already existing engineering model for the ultimate bond force, so far verified only for steel plates, is also applicable for CFRP-plates. Material-specific adaptations had to be made.

1 Introduction

The strengthening of concrete members by externally bonded steel plates is a proven technology. However, it exhibits several disadvantages such as the steel's susceptibility to corrosion in the adhesion zone and its heavy weight. Consequently, steel is increasingly replaced by thin and light CFRP laminates which exhibit excellent long-term- and fatigue- properties and corrosion behaviour. This article deals with CFRP-plates, consisting of unidirectional carbon fibers, embedded in epoxy resin matrix.

Especially at the end supports of beams and slabs, the reliable anchorage of the plate end by bond is important. For design, the ultimate bond force and the modes of failure must be known. Hence, extensive bond tests were performed. On basis of the results an engineering model of bond strength was developed.

2 Materials

The Young's modulus of carbon fibers is in the range of 240-900 GPa, their tensile strength of 2000-7000 MPa. The stress-strain behaviour is linear-elastic. In CFRP-plates, the fibers are embedded in an epoxy resin with a tensile strength of 60-90 MPa and an ultimate strain of 3 -5%. For more information see [1].

Unidirectional CFRP-plates with a fiber volume ratio of 60 - 70% are 1,0 - 1,5 mm thick and 50 - 100 mm wide. They have a tensile strength of 2000 - 3000 MPa and an E-modulus of 150 - 230 GPa. CFRP-plates are, as the fibers, linear-elastic unto failure. The contribution of the epoxy matrix to strength and Young's modulus is negligible. The short time strength is the relevant design resistance.

3 Principle of the Strengthening Method

The CFRP-plate is an additional and staggered tension chord. The behaviour of the strengthened member can be described by the truss analogy TA. Consequently, this analogy requires in the case of beams external plate stirrups, anchored in the compression zone. Such stirrups can only be realized by glued steel plates. Because the CFRP-plate will usually end before the axis of end

supports, the plate's force has to be anchored in the tension zone of the bending member. Fig. 1 shows schematically the lines of the tensile forces of the internal and external reinforcement according to the TA as well as the plate force to be anchored outside of the line of plate force. Experiments proved, that the flexural design of plate strengthened beams and slabs can be carried out following the rules for reinforced concrete. The strain limit of CFRP-plates has to be chosen in such a way, that the premature separation of plate from concrete is obviated. The shear design of plate-strengthened members also follows the principles for reinforced concrete.

4 Bond Zones of a Plate-Strengthened Concrete Member

In a plate-strengthened member, three zones of bond stress exist (Fig. 1):

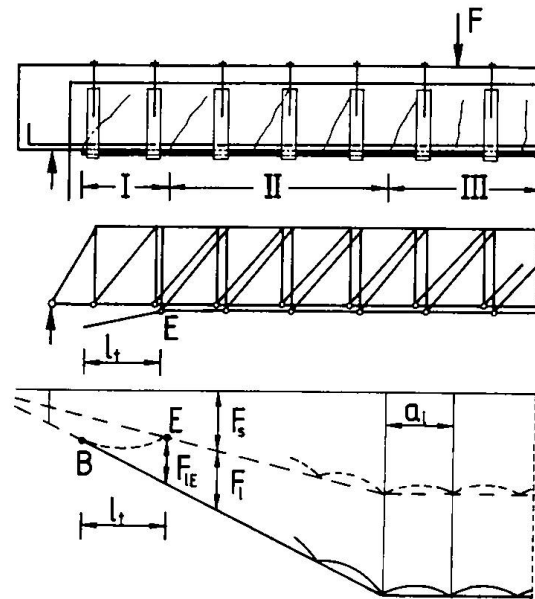


Fig.1 Truss model of a plate-strengthened beam, tensile forces according to TA and bond zones

I Anchorage of the plate end

Tensile stresses are rapidly being transferred to the plate via bond stresses, beginning at the plate end, until at the end E of the anchorage length the plate is fully connected, i.e. its share of total tensile force is equal to its share of the total reinforcement stiffness.

II Zone of shear forces and moderate bending moments

Bond stresses are caused by the variation of bending moment along the beam and by force transfer at cracks.

III Zone of high bending moments and low shear forces

In the zone of strain, bond stresses are mainly caused by force transfer at cracks.

Within the anchorage length l_t the plate end has to be anchored to the concrete for the relevant plate force F_{iE} , by high bond stresses.

5 Bond Tests

5.1 Test Methods

For the investigation of the bond behaviour of a plate end, bond tests are necessary. There are two basic types of bond tests. Volkersen /2/ and Ranisch /3/ used double-lap specimens, in which

both, the concrete and the plate were loaded with a tensile force. The other type is carried out on specimens in which the concrete is under compression and the plate under a tensile force. This type was used by Bresson, Hilti AG and Holzenkämpfer /4/ on double-lap specimens and by Wicke/Pichler /5/ and Täljsten /6/ on single-lap-specimens. For the investigation of bond behaviour of CFRP-plates, a test method was chosen, which reflects the situation of the of the plate's end. The CFRP-plates were tested in double-lap bond tests of the compression-compression type. Fig. 2 shows the test set-up in relation to the situaton in the anchorage zone.

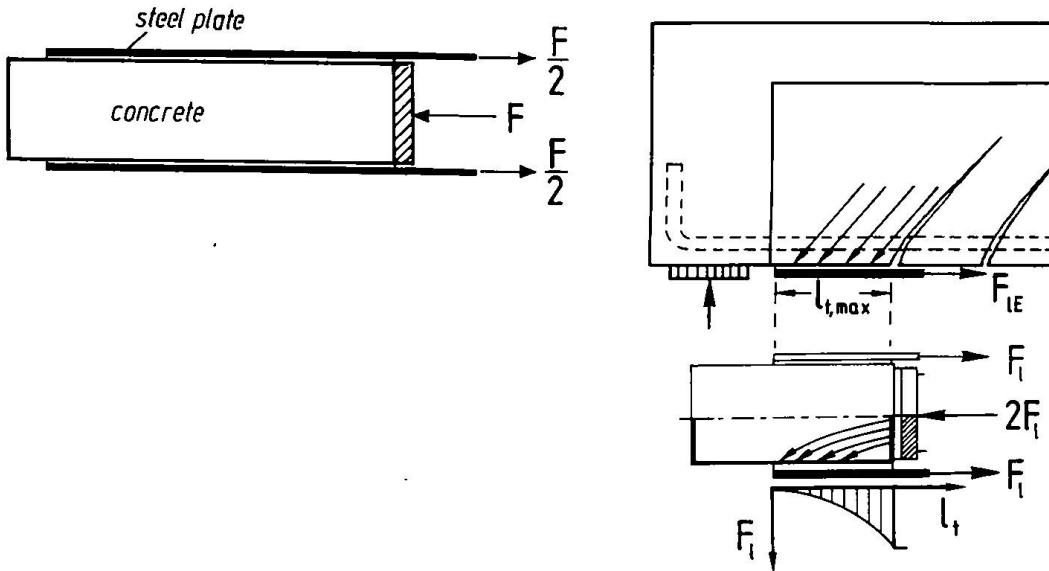


Fig. 2 Double-lap test specimen (compression-tension), used by Bresson /5/ / (left), Plate anchorage and bond test set-up (right)

5.2 The Model of Holzenkämpfer

The aim of the bond studies is, to develop an engineering model for the prediction of the ultimate bond force of a bonded CFRP-plate dependent on the relevant parameters, especially the bond length. The engineering model of the bond of glued reinforcement of /4/ is a promising on-set. This model is based on non-linear fracture mechanics. It was developed for an arbitrary elastic plate material but so far only verified for steel plates. The model is based on the differential equation of the sliding bond according to /2/and /3/:

$$\frac{d^2s_1}{dx^2} - \frac{K}{E_1 t_1} \tau(s_1) = 0 \tag{1}$$

- where: s_1: local slip between plate and concrete
- K: factor considering the stiffness ratio plate/concrete
- E_1: modulus of elasticity of the plate
- t_1: thickness of the plate
- $\tau_1(s_1)$..: bond stress as a function of s_1
- x : coordinate

The bond law $\tau_1(s_1)$ used by /4/ is shown in Fig. 3. Its ascending branch represents linear elasticity, the descending branch the softening of bond by bond cracks. The total area enclosed is the fracture energy G_f for crack initiation, which can be expressed as a function of the concrete's tensile strength.

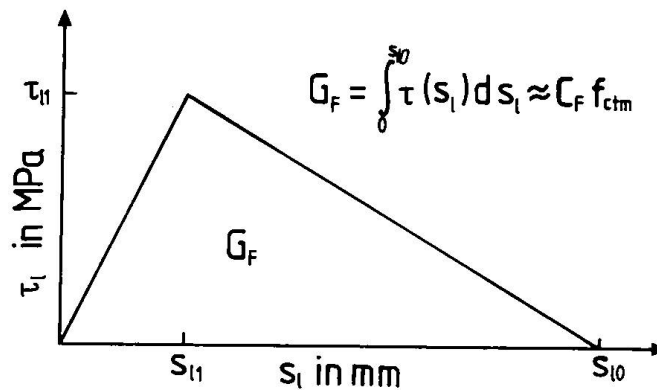


Fig. 3 Idealized local bond law of Holzenkämpfer /4/

Pre-supposing the Mohr-Coulomb criterion for bond failure, the value τ_{l1} is expressed as a function of the concrete's surface tensile strength f_{ctm} . The slips s_{l1} and s_{l0} were derived from the deformation of a representative volume of bond zone. Tests show, that the ultimate bond force increases with bond length. However, after a specific bond length $l_{t,max}$ no further increase beyond the maximum ultimate bond force T_{max} can be attained (s. Fig. 5). The following expressions are derived in /4/:

$$T_{max} = 0,40 k_b k_c b_l \sqrt{E_l t_l f_{ctm}} \quad [N] \quad (2)$$

$$l_{t,max} = \sqrt{\frac{E_l t_l}{4f_{ctm}}} \quad [mm] \quad (3)$$

The factors k_b and k_c consider influences of the plate width relative to concrete member's width and of the condition of the concrete surface. The product $k_b k_c$ usually does not differ much from 1,0. Eq. (2) is assumed to be valid for any elastic plate material, but was calibrated for steel plates. Hence, it became necessary to investigate the applicability of Eq. (2) for CFRP-plates.

5.3 Test Program, Types of Failure and Results

In all 51 bond tests were performed. The following parameters were varied: bond length l , plate width b_l , plate thickness t_l , concrete cube strength. The Figs. 4 and 5 show the results.

In all tests a sudden, brittle bond failure occurred. Two main failure types are to be distinguished, which in some cases occurred together in the same plate:

1. Concrete tensile failure 1-7 mm deep in the concrete subbase T1. The adhesive layer together with aggregate particles remained on the plate.
2. Interlaminar plate failure T2. The fibers closest to the adhesive surface were ripped out of the matrix and remained in the adhesive layer on the concrete. In most cases, interlaminar plate failure occurred after a few centimeters of concrete failure T1, which started from the loaded end of the bond length.

There was a clear dependence of the failure type on concrete strength. In concrete B25, 85% of all failures were of the Type 1 over the full bond length and 15% were a combination of T1 and T2, with T1 starting at the loaded end, as described above. In concrete B55 the combination T1/T2 with 95% clearly prevailed.

For the comparison of Holzenkämpfer's Eq. (2) with the test results, the actual concrete's surface tensile strength f_{ctm} was determined on the bond test specimens. Then, the dependence of the fracture energy had to be determined. Evaluation led to the following equations:

$$T_{Cm,max} = 0,75 k_b b_l \sqrt{E_l t_l f_{ctm}} \quad [N] \quad (4)$$

$$l_{Ct,max} = \sqrt{\frac{E_l t_l}{1,43 f_{ctm}}} \quad [mm] \quad (5)$$

Fig. 4 shows the measured ultimate bond forces $exp T_u$ plotted against the calculated ultimate bond forces $cal T_m$. For bond lengths l_t with $l_t < l_{Ct,max}$, the ultimate bond force was calculated according to /4/:

$$T_{Cm} = T_{Cm,max} \frac{l_t}{l_{Ct,max}} \left(2 - \frac{l_t}{l_{Ct,max}} \right) \quad (6)$$

The calculated values reasonably agree with the measured ones. In Fig. 5 the normalized measured and calculated ultimate bond forces, dependent on bond length are shown. The relative good agreement for most cases as well as the fact, that there exists a maximum ultimate bond force can be seen.

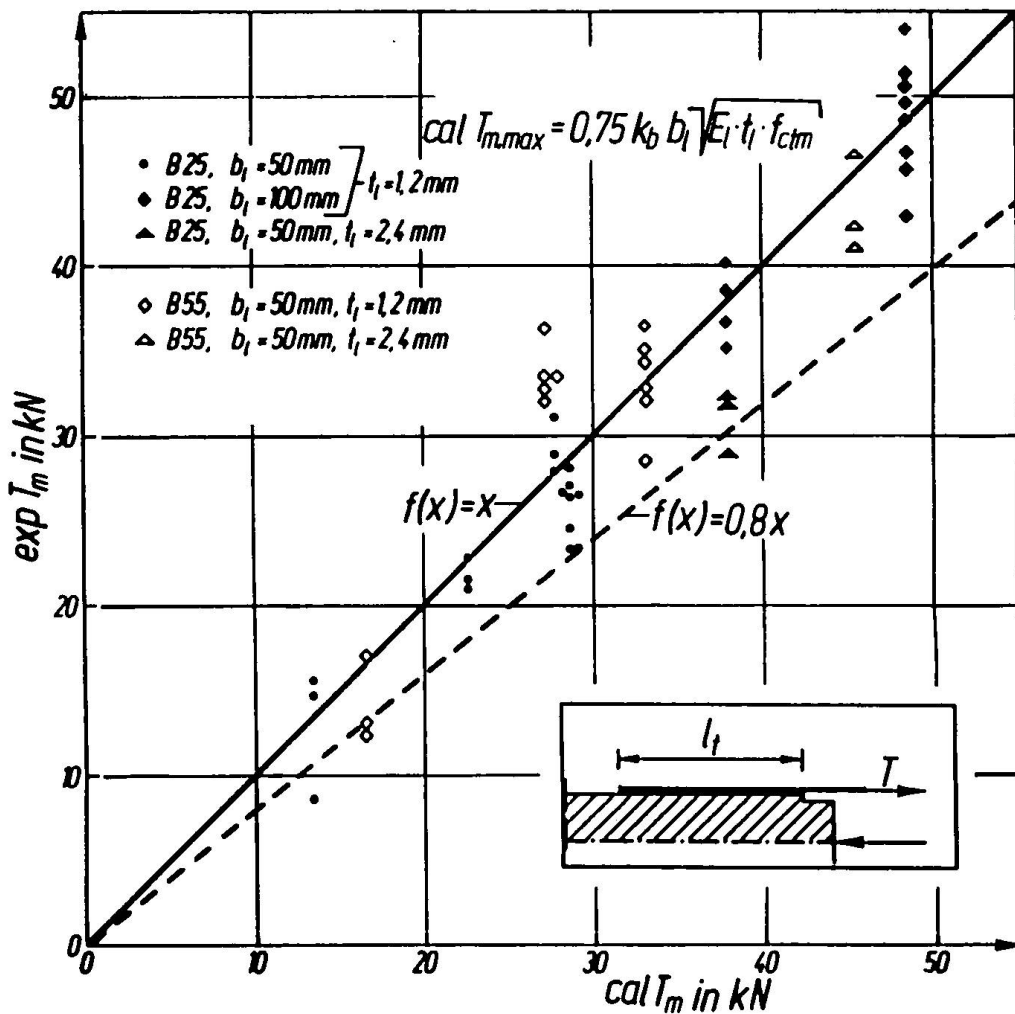


Fig.4 Calculated and measured ultimate bond forces

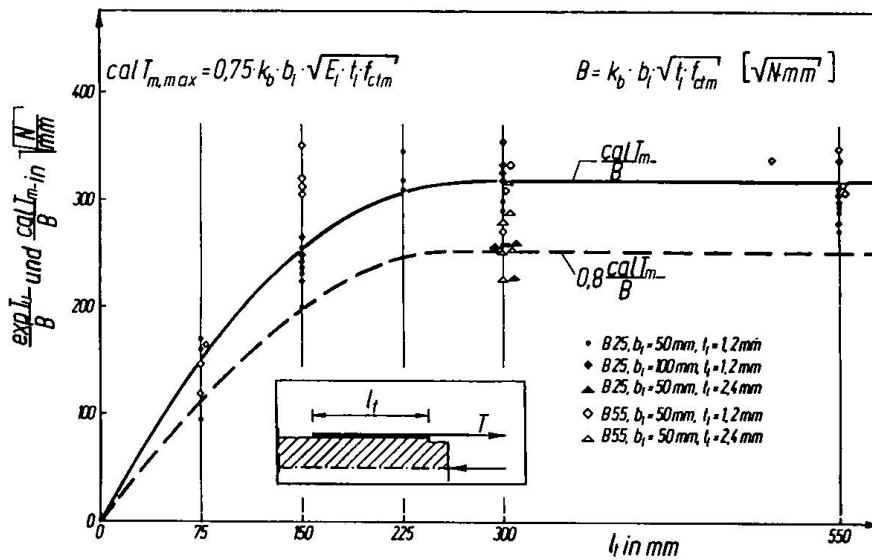


Fig. 5 Calculated and measured ultimate bond forces, dependent on the bond length

6 Conclusions

The engineering of Holzenkämpfer is also valid for CFRP-plates. The test results indicated, that this not only applies to plates with a complete failure in the concrete subbase but also to plates with a combination of concrete- and interlaminar plate failure. Despite of the different failure types the same fracture mechanism, dependent on the fracture energy, seems to be responsible for the start of a bond failure. The interlaminar plate failure is probably a secondary effect, caused by high local tensile stresses (peeling effect).

The modified formula for the ultimate bond force is an appropriate tool for the design of the plate end anchorage. It should be mentioned, that despite some previous research, there are some more important questions about the bond anchorage of CFRP-plates to be solved, e.g. the beneficial effect of plate stirrups on the ultimate bond force and the negative effect of vertical displacements of shear cracks.

Literature

- /1/ Nachträgliches Verstärken von Bauwerken mit CFK-Lamellen; Referate und Beiträge zur EMPA/SIA-Studientagung vom 21. September 1995 in Zürich; Dokumentation SIA D 0128.
- /2/ Volkersen, O.: Die Nietkraftverteilung in zugbeanspruchten Nietverbindungen mit konstanten Laschenquerschnitten, Luftfahrtforschung 15 (1938)
- /3/ Ranisch, E.-H.: Zur Tragfähigkeit von Verklebungen zwischen Baustahl und Beton - Geklebte Bewehrung. Dissertation, Institut für Baustoffe, Massivbau und Brandschutz, TU Braunschweig
- /4/ Holzenkämpfer, P.: Ingenieurmodell des Verbunds geklebter Bewehrung für Betonbauteile. Dissertation TU Braunschweig.
- /5/ Pichler, D.: Die Wirkung von Anpreßdrücken auf die Verankerung von Klebelamellen. Dissertation, Universität Innsbruck Institut für Betonbau, 1993
- /6/ Täljsten, B.: PLATE BONDING, Strengthening of Existing Concrete Structures with Epoxy Bonded Plates of Steel or Fibre Reinforced Plastics, Doctoral Thesis, Lulea 1994

Strengthening of Structures with Carbon Fibre Laminates

Werner STEINER
Civil Engineer ETH/SIA
SIKA AG
Zürich, Switzerland

Werner Steiner, born 1943, received his civil engineering degree from the ETH in Zürich. He worked several years in South Africa designing harbour structures in Durband and afterwards as project manager for a Swiss general contractor carrying out turnkey projects. After joining the Sika Group he specialised in rehabilitation work, developing the new strengthening method with CFRP-material from 1994.

Summary

Carbon fibre reinforced plastics (CFRP strips), are used ever more for the strengthening of concrete structures. The particular characteristics of CFRP strips, the most important properties of the epoxy adhesive as well as the application are described in this paper. Particular attention is given to quality assurance aspects. Application examples show that strengthening with CFRP strips is particularly well suitable for bridges.

1. Introduction

Maintenance, rehabilitation, transformation and extension of existing structures becomes ever more important in times when the number of new structures decreases. Investments for renovation of existing structural substance have kept increasing for the last 10 years. Intensive usage, manifold environmental influences and ageing affect the fitness for use and safety of structures. The main reasons that non-corroding CFRP strips have lately been used more and more often for strengthening work, are the ease of handling and the efficiency of application of the feather-light and flexible material.

2. CFRP strips

A CFRP strip, 50 mm wide and 1,2 mm thick, consists of 2,5 million carbon fibres with a diameter of one five thousandth of a millimetre. The fibres are aligned lengthways parallel by pulltrusion and bonded together with epoxy resin. The dispersion of the values of the tensile strength is small because of the large number of unidirectional fibres. Whenever a fibre in a strip breaks the remaining fibres remain intact and the rupture does not propagate as in a

homogeneous material. The embedding of the carbon fibres in the epoxy matrix assures that a broken fibre has full load bearing capacity again at few millimetres both sides of the rupture. CFRP strips behave linear-elastic up to the point of failure. Using different carbon fibres allows to manufacture CFRP strips with different modules of elasticity. For the time being, three different types of CFRP strips are used. They are available in different widths between 50 mm to 120 mm and thickness of 1,2 mm and 1,4 mm.

	Sika CarboDur S	Sika CarboDur M	Sika CarboDur H
E-modulus	155'000 N/mm ²	210'000 N/mm ²	300'000 N/mm ²
Tensile strength	>2'400 N/mm ²	>2'000 N/mm ²	>1'400 N/mm ²
Elongation at break	>1,9%	>1,1%	>0,8%

The chemical resistance of CFRP strips against pollutants generally present in the environment of structures is very good. The carbon fibres and the epoxy matrix are long-time resistant against concrete pore water, de-icing salts and hydrous acid solutions.

3. Epoxy adhesive

Two component epoxy resin systems are particularly well suitable for the bonding of CFRP strips to concrete, steel wood or bricks. This type of adhesive has very high mechanical strengths as well a good chemical resistance against aggressive media. Good wetting properties on concrete, wood etc. assure good bond characteristics.

The function of the adhesive layers is above all to transfer the forces acting onto the joined elements. Of particular importance is the elimination resp. the reduction of stress peaks. The more a layer of adhesive is able to level such stress peaks, the greater the load transferring portion of the bonded area will be.

The following properties are important for high strength structural bonding:

- High bonding forces onto elements to be joined.
- High cohesive strength of the adhesive.
- Low tendency to creep under permanent load.
- Good resistance against humidity and alkalinity.

Epoxy resin adhesive layers, thanks to their dense cross linking, meet above listed criteria very well.

Only high-quality epoxy resin adhesives should be used for the bonding of CFRP strips.

4. Application of CFRP strips

The purpose of substrate preparation is to provide optimal conditions for maximum bond with the epoxy adhesive. The removal of foreign matter and laitance is above all important.

Preparation of the substrate can be carried out applying the following methods:

- Sand blasting (best method).
- Bush hammering.
- Grinding.
- High pressure water blasting (attention: moisture).

CFRP strips should be applied at temperatures between +10°C and +35°C. The different application steps are as follows:

- Reprofilling of defective and uneven areas with epoxy mortar the previous day.
- Visual checking of the strips for mechanical damages.
- Checking the straightness of strips to be placed side by side.
- Checking the length of the CFRP strip against the length of the structural part to be strengthened.
- Cleaning of the strip's face to be bonded.
- Delimitation of the concrete surface to receive the adhesive with masking tape.
- Mixing of the epoxy adhesive.
- Application of a scrape coat of epoxy adhesive by steel trowel.
- Removal of the masking tape.
- Application of the epoxy adhesive in roof shape onto the CFRP strip.
- Placing of the strip onto the epoxy coated concrete and fixing by slight finger pressure.
- Pressing-on of the CFRP strip with a roller.
- Removal of excess adhesive.

The rigidity of the CFRP strips is such that they cannot be rolled-on onto excessively concave uneven areas. The thickness of the adhesive layer should in the average be 3 mm, minimum 1 mm, maximum 5 mm.

5. Strengthening of three bridges in Dresden

The three, almost 70 years old bridges near Dresden, suffered from heavy damages of the concrete cover and severe corrosion of the reinforcement steel. New structural analysis showed that, to recover full bearing capacity, structural strengthening was necessary besides extensive concrete repair and rehabilitation work.

To get the approval for the strengthening with CFRP strips for this particular case, tests have been carried out at the Technical University of Braunschweig with a steel reinforced concrete beam on a scale of 1 : 4. The main parameters, such as the shear and bending strengthening factors, elongation of the CFRP strip at the point of failure as well as the stresses in the inner reinforcement bars under dynamic load corresponded to the conditions existing in the real structure. The supposed 30% loss of steel-section of the reinforcements in the flexural tensile zone required a flexural tensile strengthening factor of $\eta_B = 1,98$.

After loading in steps up to a load $F = 45$ kN, the beam has been subjected to 2 million load alternations. After this, the loading was increased up to failure.

The calculated values and the values resulting from the tests are as follows:

calc. M_{u0} [kNm] . Ultimate bending moment calculated on the base of measured materials characteristics before strengthening.	req. M_{ud} [kNm] Bending moment under ultimate design load.	req. η_B Required bending strengthening factor.	exp. M_{uv} [kNm] Measured ultimate bending moment.	actual η_B Actual bending strengthening factor.
167	331	1,98	350	2,10

The test was able to prove that the method of strengthening with CFRP strips is suitable for the bridges in question. The stability and fitness for use for the intended usage of the three

bridges can be restored in full. According to the tests, a sufficient ductility of the structure is assured.

6. Strengthening of the Rhine bridge Oberriet-Meiningen

Extensive rehabilitation work had to be carried out on the bridge, built in 1963, crossing the border between Switzerland and Austria. Thorough investigations, including structural analysis according to today's SIA standards, had shown that the bridge deck was in need of transversal strengthening. In order to assure structural safety for today's traffic loads, it was decided for one thing to increase the compression zone of the bridge deck and for another to strengthen the tension zone with CFRP strips.

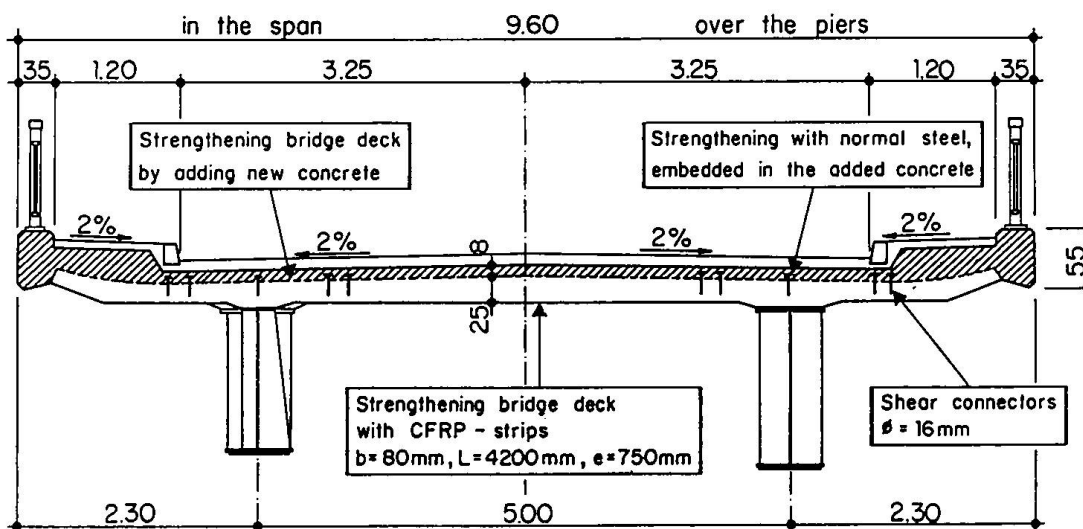


Fig. 1 Cross-section

By adding 8 cm height to the deck, it was possible to remove the chloride contaminated concrete layer by high pressure water blasting and replace it. The structural safety of the deck slab was insufficient, between as well as over the girders. The zones with negative bending moments have been strengthened with conventional steel S 500 embedded in the added concrete. The tension zone has been strengthened with CFRP strips 80 mm wide, 1.2 mm thick. A total of 160 strips, about 4.20 m long have been bonded at 75 cm intervals. The total strengthening factor of 2.4 is the result of added concrete (factor 1.4) and CFRP strips (factor 1.7).

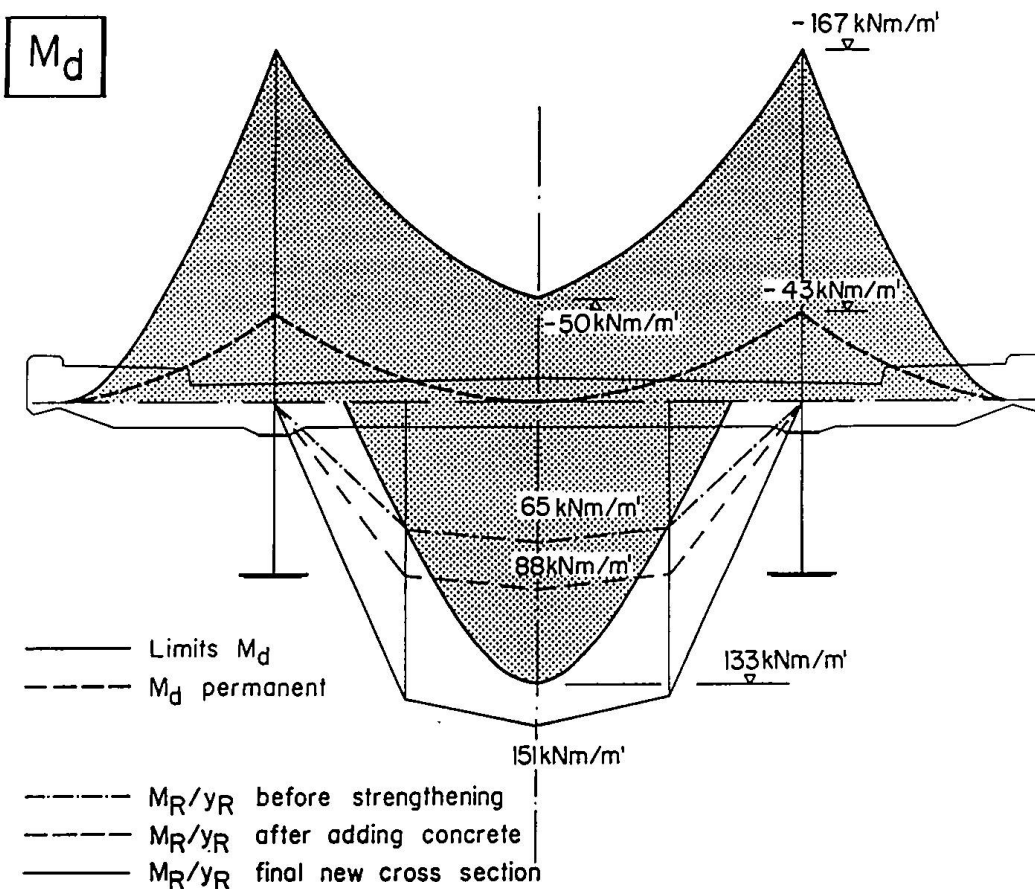


Fig 2. Transversal bending moment in bridge deck

7. Quality assurance

After preparation of the substrate, the surface is inspected visually for weak areas, inclusions in the concrete and cracks. The evenness of the concrete surface is checked with a metal batten and unevenness should not exceed 10 mm on a length of two metres.

Tensile bond strength of the concrete surface is measured by pulling off glued-on steel disks. Before starting bonding operations, ambient temperature, relative humidity of the air, dew point, temperature of concrete and CFRP strips as well as humidity of the concrete have to be measured in order to prevent imperfect bond of the adhesive due to humidity.

During bonding operations, at least 2 prisms 40 x 40 x 160 mm of the epoxy adhesive used have to be prepared per day for later testing of compressive and tensile bending strength. For each different batch of adhesive used within one day, two additional prisms have to be prepared and tested.

The quality of the bond of the applied CFRP strips is of utmost importance. Therefore, for testing purposes, some CFRP strips, longer than required by the design, are applied. Tensile bond strength tests can then be performed on this additional length. This method allows to spread the testing over a period of years.

All CFRP strips have to be checked for hollow spots by careful tapping. Concave bends may not exceed 10 mm on a length of two metres. There is no objection to convex bends pressing the strip under traction against the concrete.

8. Conclusions

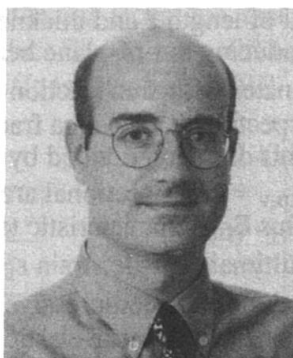
Intensive usage, manifold environmental influences and ageing affect the fitness for use of structures and their structural safety. CFRP strips, because of their outstanding properties, are used more and more for strengthening work. Their excellent long-time resistance, high corrosion resistance and light weight are particularly worth mentioning. These properties as well as the efficient way of application, the ease of executing crossings, the absence of construction joints are advantages outweighing the relatively high costs of the material. The two reported examples show that this method of strengthening is very well suitable for the strengthening of bridges.

References

1. Habennicht G., 1990: Bonding Basics, Technology, Applications
2 nd edition, Springer publishers, Berlin
2. Deuring M., 1994: CFRP strips in the construction industry
Strengthening of concrete structures.
SI+A, no 26, June 26 th 1994
3. Meier U., 1994: Strengthening of structures with fibre reinforced composite materials.
VDI - Report no 1080, 1994, pages 587 - 594.
4. Steiner W., 1995: Application practice by roll-on method, quality assurance.
SIA Documentation no D 0128
5. Meier U., 1995: Properties of unidirectional CFRP strips.
SIA Documentation no D 0128
6. Steiner W., 1996: Strengthening of structures with CFRP strips,
Advanced Composite Materials in Bridges and Structures, Montreal, Quebec, 1996
7. Walser R., Steiner W., 1996: Strengthening of the Rhine bridge Oberrriet - Meiningen
SI+A no 4, October 24 th 1996
8. Neubauer U., Rostasy F. S., 1996:
Subsequent strengthening of concrete structural parts with bonded strip of carbon fibre reinforced plastics.
Materials Science and Restoration, volume III, Aedificativ Publishers.

Behaviour of Masonry Structures Strengthened with Composites

Thanasis TRIANTAFILLOU
 Assist. Prof. of Civil Engineering
 University of Patras
 Patras, Greece



Thanasis Triantafillou, born 1963, received the Diploma in civil engineering (1985) from the University of Patras, Greece, and the MSc (1987) and PhD (1989) degrees in civil engineering from the Massachusetts Institute of Technology, where he served as Assistant Professor from 1990-93.

Summary

The paper presents a systematic analysis for the short-term strength of masonry walls strengthened with externally bonded fibre reinforced polymer (FRP) laminates, under monotonic out-of-plane bending, in-plane bending and in-plane shear, all combined with axial load, within the framework of modern design codes such as Eurocode 6. The results are presented in the form of both design equations and normalized interaction diagrams.

1. Introduction and background

Many of the masonry structures throughout the world (including several of considerable historical and architectural importance) have suffered from the accumulated effects of inadequate construction techniques and materials, seismic and wind loads, foundation settlements and environmental deterioration, and are structurally deficient or marginal for current use. In addition to these factors, changed usage and more stringent seismic design requirements have resulted in many masonry structures being designated in need of upgrading through strengthening. Traditional methods, such as reinforced concrete or shotcrete jacketing, for strengthening of masonry structures, suffer from a few disadvantages (considerable additional weight, change of dimensions, increased labour costs, obstruction of occupancy and violation of aesthetics), so that researchers have recently looked at other techniques, involving the use of fibre reinforced polymer (FRP) composites. These materials, which are typically made of carbon, glass or aramid fibres, bonded together with a polymeric matrix (epoxy, polyester, vinylester), offer the designer an outstanding combination of properties, including high strength and stiffness in the direction of the fibres, immunity to corrosion, low weight and availability in the form of laminates, fabrics and tendons of practically unlimited lengths.

Past studies related to the use of composites as strengthening materials of masonry are reported in [1-7]. These materials have been examined in the form of either unbonded tendons [1-2] or epoxy-bonded laminates or fabrics [3-7]. The last concept involves bonding of FRP strips or fabrics to the surface of masonry walls, playing the role of tensile reinforcement; the concept has been verified experimentally and applied successfully to strengthen some of the load-bearing walls of a six storey residential building in Zurich [4]. The results obtained from the above studies point to the conclusion that for the sake of both economy and optimum mechanical response, unidirectional FRP reinforcement in the form of laminates (or fabric strips) is preferable than two-dimensional fabrics which cover the whole surface of masonry walls.

In this study, the author aims at contributing to the development of a basic understanding of the mechanical behaviour of unreinforced masonry walls strengthened with externally bonded composite laminates (or fabric strips) using simple modelling, consistent with the approach of Eurocode 6 for masonry structures. The three most common cases of masonry loading are analyzed, namely: out-of-plane bending, in-plane bending and in-plane shear (with axial force in all cases).

2. Analysis

2.1 Out-of-Plane Bending With Axial Force

Consider first the case of a masonry wall of length ℓ and thickness t , subjected to compressive force N_{Rd} and bending moment $M_{O,Rd}$ inducing out-of-plane bending. The wall's tensile face is reinforced with epoxy-bonded FRP laminates with area fraction equal to Q_v and Q_h in the longitudinal and transverse direction, respectively. The area fraction in one direction is defined as the total cross-sectional area of FRP in this direction divided by the corresponding area of the wall. Hence Q_v is equal to $A_{frp,v}/\ell t$, where $A_{frp,v}$ = cross-sectional area of FRP in longitudinal direction. The FRP laminates have Young's modulus E_{frp} , characteristic tensile strength (that is, with a 5% probability of under-strength) $f_{frp,k}$ and ultimate tensile strain $\epsilon_{frp,u}$; and the masonry has characteristic compressive strength f_k and ultimate compressive strain $\epsilon_{M,u}$. As far as stress-strain relationships are concerned, the FRP is considered linear-elastic to failure and the masonry is idealized according to the rectangular compressive stress block approach. The partial safety factors for masonry and FRP are denoted as γ_M and γ_{frp} , respectively. Further assumptions are that plane sections before bending remain plane after bending and that the tensile resistance of the masonry, the adhesive and the FRP in the transverse direction may be neglected.

Typically, failure of the FRP-strengthened masonry will be due to compressive crushing, unless the longitudinal reinforcement area fraction, Q_v , is very small. In the latter case, FRP fracture will precede masonry crushing, and thereafter the wall will behave as unreinforced. The limiting Q_v value, $Q_{v,lim}$, for such a mechanism to be avoided, is obtained by considering the strain and stress distribution in the cross section, as shown in Fig. 1, with $\epsilon_{frp} = \epsilon_{frp,u}$ and $E_{frp}\epsilon_{frp} = f_{frp,k}/\gamma_{frp}$. Force equilibrium and strain compatibility give the following equation for the limiting FRP area fraction:

$$\omega_{lim} = \frac{\epsilon_{M,u} E_{frp}}{f_k} Q_{v,lim} = \frac{\epsilon_{M,u}}{\epsilon_{frp,u}} \left[\frac{0.8}{\gamma_M} \frac{1}{(1 + \epsilon_{frp,u} / \epsilon_{M,u})} - \frac{N_{Rd}}{\ell t f_k} \right] \quad (1)$$

Next, provided that $Q_v \geq Q_{v,lim}$, the bending capacity of the cross section can be obtained by considering compatibility of strains and equilibrium of internal forces and moments, as shown in Fig. 1. The result is given in the following form:

$$\frac{M_{O,Rd}}{\ell t^2 f_k} = \frac{1}{2} \omega \frac{(1-x/t)}{x/t} + \frac{0.4}{\gamma_M} \frac{x}{t} \left(1 - 0.8 \frac{x}{t} \right) \quad (2)$$

where

$$\frac{x}{t} = \frac{\gamma_M}{1.6} \left[-\omega + \sqrt{\omega^2 + \frac{3.2}{\gamma_M} \left(\omega + \frac{N_{Rd}}{\ell t f_k} \right)} \right] \quad (3)$$

and

$$\omega = \frac{\epsilon_{M,u} E_{frp}}{f_k} Q_v \quad (4)$$

As seen in Fig. 2 (based on $\gamma_M = 2.5$ and $\epsilon_{frp,u}/\epsilon_{M,u} = 4$), for low to moderate axial load levels, the bending capacity increases with the normalized FRP area fraction ω . Such an increase may vary from quite dramatic to negligible, depending on the axial load; and for values of ω exceeding approximately 0.5 it is, in most cases, negligible. It is also quite interesting to note that for high axial load ratios (exceeding approximately 0.3) the bending capacity decreases as ω increases. It may be observed in Fig. 2 that the upper curve, corresponding to zero axial load, does not continue all the way to $\omega = 0$. The missing part is associated with FRP fracture before crushing of

the masonry. The limiting value of ω at the transition between the two failure modes is 0.016. As given by (1), such limiting values do not exist for $N_{Rd}/\ell t f_k \geq 0.064$. Hence it may be concluded that, for practical axial load levels and FRP area fractions, premature FRP fracture is highly unlikely to occur. In addition, Fig. 2 in combination with (4) reveal that for a given masonry material the effectiveness of the strengthening technique, that is the increase in out-of-plane bending capacity, depends on the product $E_{frp}Q_v$; very stiff laminates, such as CFRP, are much more efficient than others of lower stiffness, such as GFRP.

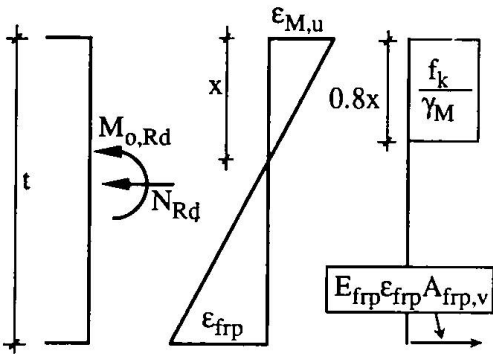


Fig. 1 Strain and stress distribution at out-of-plane flexural failure

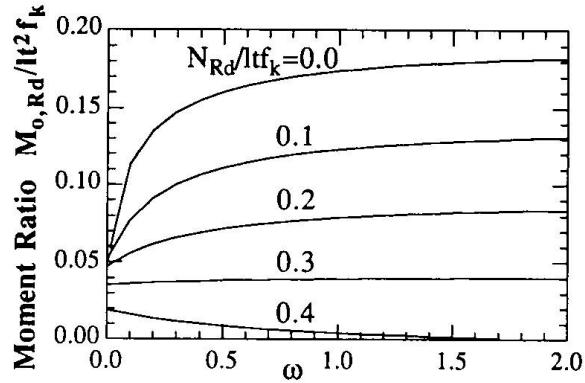


Fig. 2 Out-of-plane moment capacity versus normalized FRP area fraction

2.2 In-Plane Bending With Axial Force

Consider next the case of the FRP-strengthened masonry wall under in-plane bending moment $M_{i,Rd}$ with axial force N_{Rd} . The longitudinal tensile reinforcement is assumed to be in the form of n laminates of cross-sectional area A_i each, at an equal spacing s . Here, too, failure will be due to compressive crushing, unless: (a) Q_v is very small, which will result in premature FRP fracture (this is highly unlikely); (b) the laminates' bond development length is too short, which will result in shearing of the FRP in the tension zone (peeling-off) directly beneath the bond. Quantification of the peeling-off failure mechanism is not attempted here. Note that for the rather limited cases where in-plane flexural failure precedes in-plane shear failure (long and narrow, as opposed to squat elements), the geometry of masonry walls will most likely be such that the development length will be sufficiently large, so that failure will be dominated by compressive crushing.

The limiting Q_v value, $Q_{v,lim}$, for premature FRP fracture to be avoided, is obtained by considering the strain and stress distribution in the cross section, as shown in Fig. 3 (with $\epsilon_n = \epsilon_{frp,u}$). It can be shown that force equilibrium and strain compatibility give the following equation for the limiting FRP area fraction:

$$\omega_{lim} = \frac{\epsilon_{M,u} E_{frp}}{f_k} Q_{v,lim} = \frac{(g+1)}{(\epsilon_{frp,u}/\epsilon_{M,u} - g)} \left[\frac{0.4(g+1)}{\gamma_M} \frac{1}{(1 + \epsilon_{frp,u}/\epsilon_{M,u})} - \frac{N_{Rd}}{\ell t f_k} \right] \tag{5}$$

Under the assumption that $Q_v \geq Q_{v,lim}$, the bending capacity of the cross section can be obtained from strain compatibility and equilibrium of internal forces and moments, according to Fig. 3. After proper manipulations, the result is obtained in the following form:

$$\frac{M_{i,Rd}}{\ell^2 f_k} = \frac{(n+1)g^2}{12(n-1)} \omega \frac{1}{x/\ell} + \frac{0.4}{\gamma_M} \frac{x}{\ell} \left(1 - 0.8 \frac{x}{\ell} \right) \tag{6}$$

where

$$\frac{x}{\ell} = \frac{\gamma_M}{1.6} \left[-\omega + \frac{N_{Rd}}{\ell t f_k} + \sqrt{\left(\omega \frac{N_{Rd}}{\ell t f_k} \right)^2 + \frac{1.6}{\gamma_M} \omega} \right] \quad (7)$$

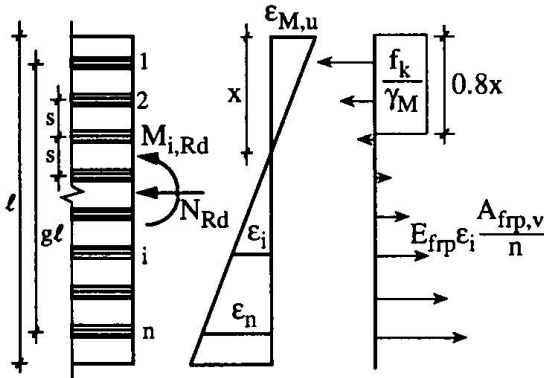


Fig. 3 Strain and stress distribution at in-plane flexural failure

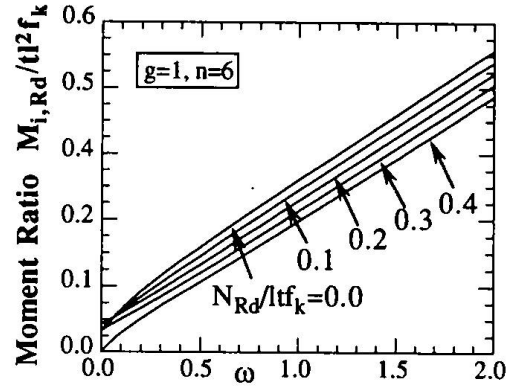


Fig. 4 In-plane moment capacity versus normalized FRP area fraction

As Fig. 4 shows, the bending capacity, in general, increases almost linearly with the normalized FRP area fraction ω (and, for a given masonry material, almost linearly with $E_{frp}Q_v$), and is considerable, regardless of the axial load level. For a given ω , higher values of moment capacity are possible as the axial load increases, but this dependence is weak.

Examination of (6) shows that the number of laminates plays an important role in mechanical response. For the same area fraction, the reinforcement's effectiveness increases by decreasing the number of laminates; using two laminates as far apart as possible results in the highest increase in bending capacity. Note that the last statement is not valid in the case of steel-reinforced masonry, where the in-plane moment capacity is almost independent of whether the reinforcement is uniformly distributed along the wall or concentrated near the ends.

2.3 In-Plane Shear With Axial Force

Last, we examine the case of FRP-strengthened masonry walls under in-plane shear V_{Rd} with axial force N_{Rd} . According to Eurocode 6 [8], the analysis and design of reinforced masonry in shear is based on the assumption that the total contribution to shear capacity is given as the sum of two terms, similarly to reinforced concrete. The first term, V_{Rd1} , accounts primarily for the contribution of uncracked masonry, while the second term, V_{Rd2} , accounts for the effect of shear reinforcement, which is usually modeled by the well-known truss analogy:

$$V_{Rd} = V_{Rd1} + V_{Rd2} \leq \frac{0.3 f_k t d}{\gamma_M} \quad (8)$$

where $V_{Rd1} = f_{vk} t d / \gamma_M$ and d is the effective depth. For masonry walls with several layers of reinforcement, as in our case, d can be taken approximately equal to 0.8ℓ [9]. f_{vk} is the characteristic shear strength of masonry, given as:

$$\begin{aligned} f_{vk} &= \min \left[f_{vko} + 0.4 \frac{N_{Rd}}{\ell t}, 0.7 f_{vk,lim}, 0.7 \max(0.065 f_b, f_{vko}) \right] \\ &= \min \left(f_{vko} + 0.4 \frac{N_{Rd}}{\ell t}, f_{vk,max} \right) \end{aligned} \quad (9)$$

where: f_{vko} , the characteristic shear strength of masonry under zero compressive stress, is between 0.1-0.3 MPa (the lower limit applies in the absence of experimental data), depending on the type of masonry units and the mortar strength; $f_{vk,lim}$, the limiting value of f_{vk} , is in the order of 1.0-1.7 MPa, depending on the type of masonry units and the mortar strength; f_b , the normalized compressive strength of masonry units, is equal to a size factor (between 0.65-1.55) times the mean compressive strength of masonry units; and the factor 0.7 applies only in the (usual) case of seismic design. Note that if strengthening is applied in the absence of full repair, that is in the case of damaged (diagonally cracked) masonry walls, the value of f_{vk} should be taken lower than that given by (9). Such a reduction depends on the degree of damage, and can only be estimated on a case by case basis.

The contribution of FRP reinforcement to shear capacity is more difficult to quantify. One assumption made here is that the contribution of vertical FRP reinforcement, which provides mainly a dowel action effect, is negligible. This can be justified by the high flexibility of the laminates, in combination with their local debonding in the vicinity of shear cracks. The only shear resistance mechanism left is associated with the action of transverse laminates, which can be modeled in analogy to the action of stirrups in reinforced concrete beams. Adopting the classical truss analogy, it can be shown that the contribution of transverse FRP to shear capacity is:

$$V_{Rd2} = Q_h E_{frp} \left(r \frac{\epsilon_{frp,u}}{\gamma_{frp}} \right) t 0.9d = \frac{0.7}{\gamma_{frp}} Q_h E_{frp} \epsilon_{frp,e} \ell t \quad (10)$$

where r is a reinforcement efficiency factor, depending on the exact FRP failure mechanism (FRP debonding or tensile fracture), γ_{frp} , the partial safety factor for FRP in uniaxial tension is approximately equal to 1.15, 1.20 and 1.25 for CFRP, AFRP and GFRP, respectively [2], and $\epsilon_{frp,e}$ is an effective FRP strain, the only unknown yet to be determined for completing the analysis on FRP contribution to shear capacity. Qualitatively, one may argue that $\epsilon_{frp,e}$ depends heavily on the area of the FRP-masonry debonded interfaces, or, in other words, on the FRP development length, defined as that necessary to reach FRP tensile fracture before debonding. Apart from the bond conditions, the development length depends (almost proportionally) on the FRP axial rigidity (area times elastic modulus), expressed by the product $Q_h E_{frp}$. Hence, one would roughly expect $\epsilon_{frp,e}$ to be inversely proportional to $Q_h E_{frp}$. The implication of this argument is that as the FRP laminates become stiffer and thicker debonding dominates over tensile fracture and the effective FRP strain is reduced.

From all the above, we can finally write the shear capacity of FRP-strengthened masonry as:

$$\frac{V_{Rd}}{f_k \ell t} = \frac{0.8}{\gamma_M} \min \left(\frac{f_{vko}}{f_k} + 0.4 \frac{N_{Rd}}{f_k \ell t}, \frac{f_{vk,max}}{f_k} \right) + \frac{0.7}{\gamma_{frp}} \omega_h \frac{\epsilon_{frp,e}}{\epsilon_{M,u}} \leq \frac{0.25}{\gamma_M} \quad (11)$$

where $\omega_h = \epsilon_{M,u} E_{frp} Q_h / f_k$. The expression for $\epsilon_{frp,e}$ has recently been obtained for concrete members strengthened with FRP in shear in [10]. The same expression is adopted here for masonry structures, and given below:

$$\epsilon_{frp,e} = 0.0124 - 0.0214(Q_h E_{frp}) + 0.0107(Q_h E_{frp})^2 \quad (12)$$

where E_{frp} is in GPa.

To obtain a better insight of the FRP contribution to the shear capacity of masonry walls, the results given above are presented in Fig. 5 for typical cases of material properties, as follows: $\epsilon_{M,u} = 0.0035$, $\gamma_M = 2.5$, $f_k = 5$ MPa, $\gamma_{frp} = 1.15$, $f_{vko} = 0.2$ MPa, $f_{vk,max} = 0.5$ MPa (Fig. 5a) and $f_{vk,max} = 1.0$ MPa (Fig. 5b). It is demonstrated that, depending on the axial load level, the

increase in shear capacity due to the external reinforcement can be high, and that it reaches a cut-off value at relatively low values of ω_h , corresponding to very low values of FRP area fractions.

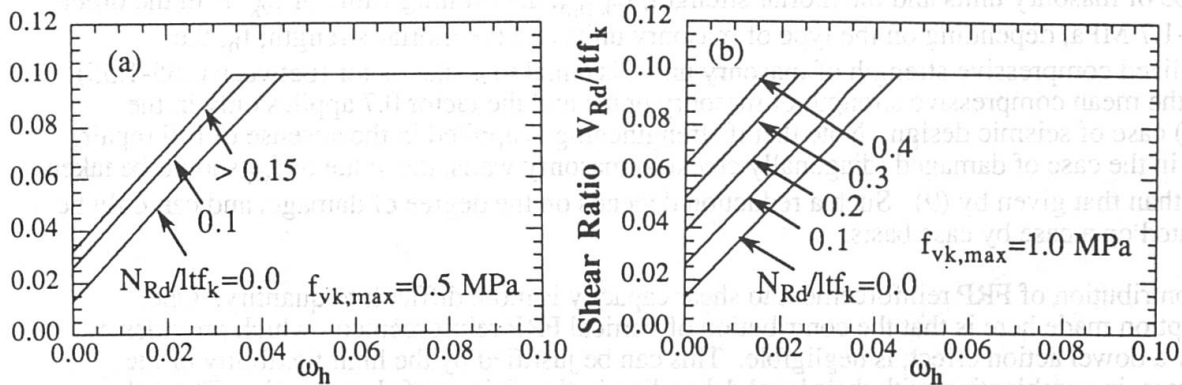


Fig. 5 In-plane shear capacity versus normalized FRP area fraction

3. Conclusions

Strengthening of masonry walls with externally bonded FRP laminates appears to be an attractive alternative to traditional retrofit techniques, especially in cases where implementation of such techniques is impractical. The present study focused on establishing a systematic analysis procedure for the short-term strength of FRP-strengthened masonry walls under monotonic out-of-plane bending, in-plane bending and in-plane shear, all combined with axial load, within the framework of Eurocode 6. It was shown that when out-of-plane bending response dominates, which is typically the case in the upper levels of masonry structures (where axial loads are low), the increase in bending capacity is quite high. Most important in the case of in-plane bending is the area fraction and distribution of reinforcement: high area fractions of reinforcement placed near the highly stressed zones give considerable strength increases. Finally, the in-plane shear capacity of FRP-strengthened walls can be quite high, too, especially in the case of low axial loads.

REFERENCES

1. Triantafillou, T. C. and Fardis, M. N. (1993). "Advanced composites for strengthening historic structures." *IABSE Symp. on Structural Preservation of the Architectural Heritage*, Rome, 541-548.
2. Triantafillou, T. C. and Fardis, M. N. (1997). "Strengthening of historic masonry structures with composite materials." To appear in *Materials and Structures*.
3. Schwegler, G. (1994). *Strengthening of Masonry with Fibre Composites*, Doctoral thesis, Federal Institute of Technology, Zürich (in German).
4. Schwegler, G. and Kelterborn, P. (1996). "Earthquake resistance of masonry structures strengthened with fibre composites." Ernst Basler & Partners Ltd., Internal Report.
5. Ehsani, M. R. (1995). "Strengthening of earthquake-damaged masonry structures with composite materials." In *Non-metallic (FRP) Reinforcement for Concrete Structures*, L. Taerwe editor, 680-687.
6. Laursen, P. T., Seible, F., Hegemier, G. A. and Innamorato, D. (1995). "Seismic retrofit and repair of masonry walls with carbon overlays." In *Non-metallic (FRP) Reinforcement for Concrete Structures*, L. Taerwe editor, 616-623.
7. Seible, F. (1995). "Repair and seismic retest of a full-scale reinforced masonry building." *Proc. 6th International Conference on Structural Faults and Repair*, Vol. 3, 229-236.
8. Eurocode No. 6, *Design of Masonry Structures*, Comité Euro-International du Béton, 1994.
9. Paulay, T. and Priestley, M. J. N. (1992). *Seismic Design of Reinforced Concrete and Masonry Buildings*, John Wiley & Sons, Inc., New York.
10. Triantafillou, T. C. (1997). "Shear strengthening of reinforced concrete beams using epoxy-bonded FRP laminates." To appear in the *ACI Structural Journal*.

Earthquake Resistance of Masonry Structures Strengthened with CFRP-Sheets

Gregor SCHWEGLER
Dr. sc. techn. dipl. Ing. ETH
Ernst Basler & Partner Ltd.
Zollikon, Switzerland



Gregor Schwegler, born 1963, received his civil engineering degree 1990 at the ETH in Zurich, Switzerland. His PhD was conferred on him in 1994 by the same university and the EMPA (Swiss Federal Laboratories for Materials Testing and Research), Dübendorf.

Summary

Two 60 year old, adjacent residential buildings in the city of Zurich, Switzerland, are converted into an office building. Major changes to the structural system were necessary; in particular, some load bearing walls had to be replaced or reinforced to resist potential earthquake forces. The reinforcement is carried out by carbon fiber reinforced plastic sheets (CFRP), which are glued to the existing shear wall and anchored in the RC-slabs. The efficiency of this system was confirmed by the Swiss Federal Laboratories for Materials Testing and Research EMPA.

1. Introduction

In recent years, engineers are more often faced with the reconstruction or upgrading of existing buildings rather than designing new ones. Although it would be more economical in some cases to replace a building completely, city planning regulations and historical reasons do not allow to do major changes to many buildings, especially on facades. As most of the older buildings are not designed to resist earthquake forces, architects and engineers are challenged to find economical solutions to make structural systems and the structural elements earthquake-resistant. Especially when the usage of a building is changed from living to office space and shopping areas, major changes of the structural system are required. Consequently, old structural elements are replaced by new ones, or they have to be strengthened. In many cases it is desirable to maintain as many old structural elements as possible if they can be strengthened economically, i.e. without undue interference with other remaining structures or the usage of space.

In the city of Zurich, two adjacent 60 year old residential buildings of 6 storeys are converted into one office building. Major structural changes are necessary. Old wooden slabs are replaced by RC-slabs. Load bearing masonry walls are partly eliminated and replaced by new ones. Some of the remaining load bearing masonry walls are strengthened by using carbon fiber sheets, so that the earthquake load can be resisted. The carbon fiber sheets are glued to the masonry wall and anchored in the slab. This strengthening method has been tested in full scale tests at the Swiss Federal Laboratories for Materials Testing and Research EMPA. These tests showed a significant increase in strength and ductility of the CFRP-strengthened masonry wall elements [Schwegler G. 1994a]. As it is easy to apply and economical, this strengthening method is very promising.

In the following, the application of the above mentioned method of strengthening masonry walls by CFRP-sheets is demonstrated [Ernst Basler & Partners Ltd., 1995].

2. Reconstruction Project

Two adjacent residential buildings are functionally joined so that they can be used as offices (Figure 1). All structural elements are affected by this conversion. Only a small number of them remains more or less untouched. All inner walls are removed. The outer wall on the rear side of the building is replaced by a light weight construction. The facade looking onto the main street (called Mühlebachstrasse) has to be retained. However, in the center part a large window is created (Figure 2). On the ground floor level, the load bearing walls are replaced by a new arrangement of columns to create shop windows (Figure 3). The fire protection walls separating the neighbouring buildings remain.

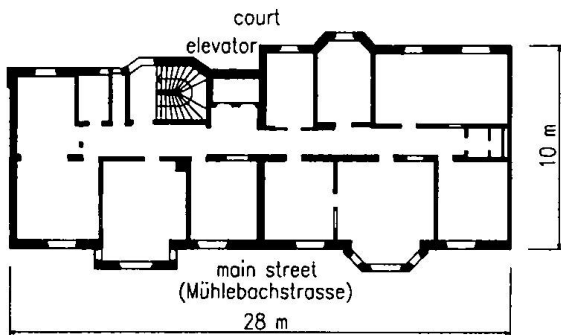


Figure 1: Existing bearing structure on 2nd floor before remodeling

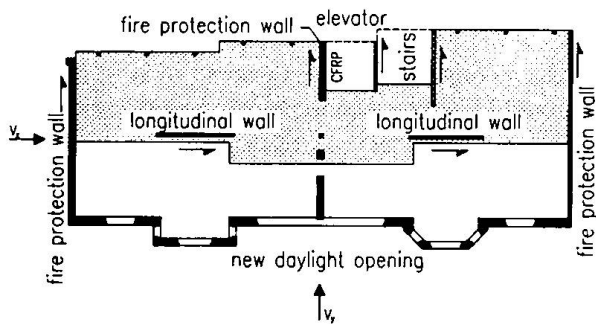


Figure 2: Bearing structure 1st to 4th floors, after remodeling

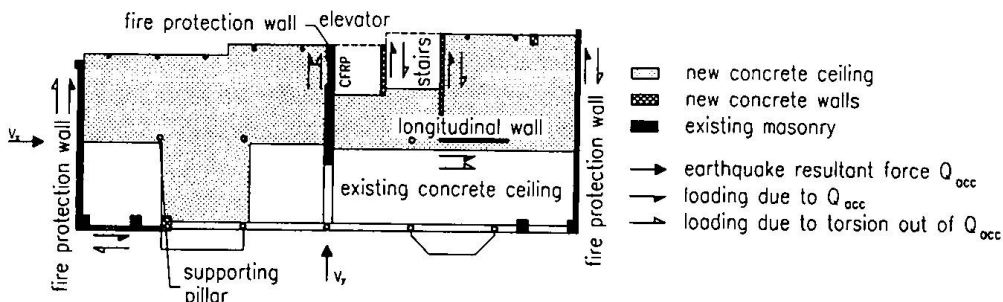


Figure 3: Bearing structure ground floor, after remodeling

These major changes to the structural system lead to a markedly different dynamic behavior than before. Both the stiffness and the strength have thus been altered, which had to be considered in the design against earthquakes.

3. Earthquake Resistance

The major horizontal earthquake forces act at the floor levels. The floor slabs have to be stiff and strong enough to transfer these forces into the shear walls, from where they are carried to the foundation. In the transverse direction of the building, the lateral resistance is provided by the shear walls of the stair case, the fire protection walls of the elevator shaft and by the double masonry wall to the adjacent buildings. In this direction, the stiffness, mass and strength are more or less symmetrically arranged (Figure 2).

In the longitudinal direction there are two load resisting walls in the center of the building from the 1st to the 4th floor. On the ground floor level, one of these two walls is replaced by an eccentric wall in the facade. Should it come to an earthquake, this leads to significant torsion in the longitudinal direction. To balance this torsion, the structural elements in the transverse direction need to be taken into account.

The existing wooden floor slabs are not rigid and not strong enough for the lateral load transfer and have thus to be partly replaced by RC-slabs. The large lateral forces on the shear walls of the elevator shaft required a strengthening which was done using carbon fiber sheets.

4. Characteristics of the CFRP Strengthening Material

The CFRP-sheets are a combination of unidirectional high strength carbonfibers and of an epoxy resin matrix. This leads to a material of high strength and stiffness. CFRP-sheets are produced in strands of unlimited length by the pultrusion-process and delivered to the site of application in rolls.

CFRP-sheets have major advantages over sheets made of steel. CFRP-sheets are superior with respect to corrosion, fatigue behavior and strength. In addition, they are light and easy to handle and simple in the application.

The most relevant material characteristics of the CFRP-sheets are shown in table 1.

Type of strengthening material	Ultimate tensile strength $\sigma_{u\parallel}$ [N/mm ²]	Young's Modulus E_{\parallel} [N/mm ²]	Ultimate tensile strain $\epsilon_{u\parallel}$ [%]
C-Fiber T700S	2400	155'000	1.90
steel	235	210'000	> 5%

Table 1: Major material properties of CFRP-sheets as compared to steel-plates

Compared to steel, CFRP shows linear elastic material properties, and the ultimate tensile strain of the applied CFRP-sheets amounts to $\epsilon_u = 1.9\%$. These material properties have to be taken into account during the planning process. The large scale tests conducted at EMPA show that with an appropriate distribution of the CFRP-sheets on the masonry wall, considerable system's ductility can be achieved [Schwegler G., 1994a, 1994b].

5. Application of the CFRP-Sheets

Before gluing the CFRP-sheets to the masonry walls, the substrate has to be freed of all loose or unsound particles, such as rendering and plaster materials, or paints and wallpapers, etc. In order to obtain a perfect straightness in the final position, all protruding surface points have to be chipped off and all surface depressions leveled out with epoxy adhesive. After applying the special epoxy adhesive to both contact surfaces, the CFRP-sheets are then fixed to the masonry wall with light hand pressure, and full contact is ensured by further pressure application with simple rubber rollers (Figure 4).

The CFRP-sheets are anchored in the adjacent RC-slabs and -walls. Thus stress concentrations in the masonry walls are thereby avoided. For each anchorage, a cavity is worked into the concrete, or core drillings are carried out. Next, the ends of the sheets are equipped with an adhesive bridge and fed into the cavities or drilling holes, before filling the holes with liquid epoxy-mortar. Thanks to this new anchorage technique, only a very short length is needed to anchor the forces in the concrete (Figure 5).

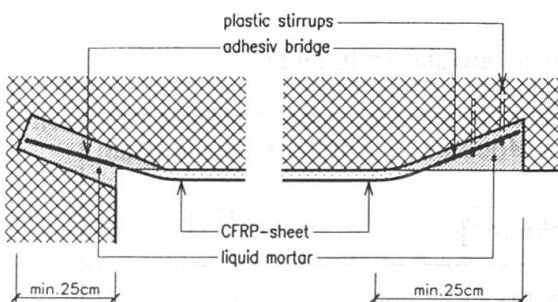


Figure 5: Anchorage of the CFRP-sheets in the concrete

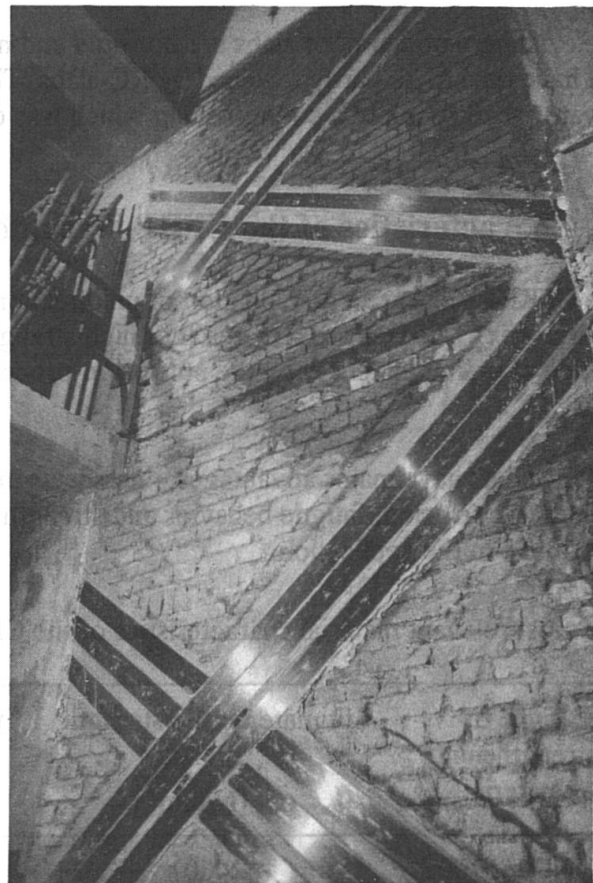


Figure 4: Distribution of CFRP-sheets on masonry shear wall

In order to limit the amount of work, the CFRP-sheets are only used on one side of the load-bearing wall. The tests at EMPA have shown that the resulting eccentricity only causes negligible effects on the strength of the shear wall.

6 Dimensioning of Reinforced Shear Walls

For dimensioning a CFRP-reinforced shear wall, the method of "stress-fields" can be used [Muttoni A., Schwartz J., Thürlimann B., 1988]. This method allows to estimate the shear wall resistance easily and with sufficient accuracy. The flow of the forces in the shear wall can be described by using truss models. The forces of each strut of the truss model correspond to the resulting inner forces. These resultants are then converted into static equivalent stress-fields. In figure 6, the course of the stress-field inside the CFRP-reinforced masonry walls is pictured. To keep the illustration simple, only one symmetrical half of the stress-fields is shown.

The horizontal forces that are acting at the floor levels together with the vertical forces in the load bearing walls lead to diagonal stress-fields which carry the compressive forces. The tensile forces are carried by the CFRP-sheets. The stresses of a stress-field are uniaxial on their whole length. In the areas of application of forces, referred to as knots, the state of stresses is biaxial. All other areas are free from stresses.

The angle between the CFRP-sheets and the vertical line should be chosen as large as possible to increase the lateral resistance. The dimensioning of reinforced load bearing masonry walls using the method of stress-fields is described more detailed in [Muttoni A., Schwartz J., Thürlimann B., 1988] and [Schwegler G., 1994a].

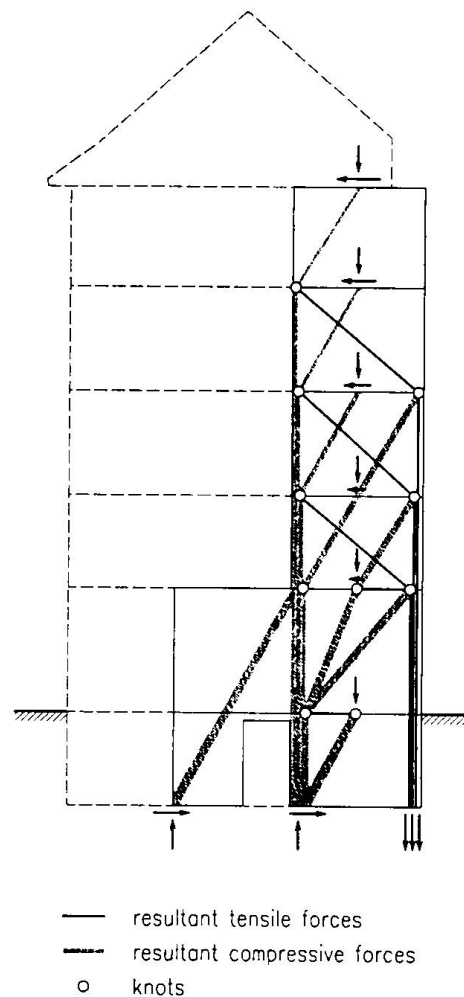


Figure 6: Stress-field of the CFRP-reinforced load bearing masonry wall

7 Conclusions

The application of CFRP-sheets to the existing load bearing masonry shear wall significantly increased its lateral resistance and ductility. Alternative methods such as reinforced shotcrete or the replacement of the wall would have been more expensive. Besides, strengthening by reinforced shotcrete would have led to an additional thickness of 700 mm, which for architectural reasons would not have been acceptable.

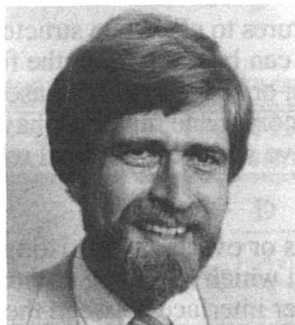
The CFRP reinforcing method for masonry walls proves to be a very efficient method in the field of earthquake resistance design, as it is economical and easy to apply.

References

- Ernst Basler und Partner AG (1995). Konkret 1995, Unternehmenspublikation 95.
Ernst Basler und Partner AG Ingenieurunternehmen, Zollikon ZH (Switzerland)
- Muttoni A., Schwartz J., Thürlimann B. (1988). Bemessung und Konstruktion von Stahlbetontragwerken mit Spannungsfeldern. Vorlesung ETHZ (Institute of Technology Zurich).
- Schwegler G. (1994a). Verstärken von Mauerwerk mit Hochleistungsfaserverbundwerkstoffen. Dissertation. Eidgenössische Materialprüfungs- und Forschungsanstalt Dübendorf, EMPA-Bericht Nr. 229.
- Schwegler G. (1994b). Masonry construction strengthened with fiber composites in seismically endangered zones. 10th European Conference on Earthquake Engineering. Vienna, Austria.

Advanced Composites for Bridge Infrastructure Rehabilitation and Renewal

Frieder SEIBLE
Professor and Chair
Univ. of California, San Diego
La Jolla, CA, USA



Frieder Seible received his civil engineering degrees from the Universities of Stuttgart, Calgary and Berkeley. He is director of the Powell Structural Research Laboratories. His research focus is on bridge design, seismic design and retrofitting of bridges, large scale experimental testing and the application of advanced composites in civil engineering.

Summary

Recent developments in new bridge systems using advanced composite (polymer matrix composite) materials and manufacturing technologies have shown that while these new bridge systems are technically feasible, they are not yet economically competitive. However, the combination of these new advanced composite materials with conventional structural materials such as concrete and steel can result in new composite design and construction concepts which are both structurally and economically efficient.

1. Introduction

Deterioration of our aging bridge inventory, wear from service and environmental loads, as well as ever increasing allowable or legal loads require accelerated rehabilitation and renewal programs to maintain even current service levels on our bridge infrastructure network. Demands for longer service life, increased durability and reduced maintenance have prompted a new look at advanced composite materials such as glass, aramid and carbon fibers embedded in a polymer matrix to provide due to their chemical inertness, high mechanical characteristics, and light weight, some of the above performance requirements.

To date advanced composite materials have been used very effectively in the repair and strengthening of existing concrete bridges and in the seismic retrofit of bridge columns, bridge superstructures and shear walls. The main advantages are derived from the light weight of these new materials in the form of easy handling during installation at insignificant increases in weight and structural dimensions. The strengthening applications to date consist either of epoxy bonding of cured pultruded laminates [1] or of wet lay-up fabrics onto the concrete substrate [2], creating a new composite structure.

Attempts to manufacture complete advanced composite replacement members or complete bridge systems [2, 6] have shown that all-advanced composite structural systems are certainly feasible with current materials and manufacturing technologies, but while technically sound and structurally reliable these new members or systems have, economically, a difficult time to compete with conventional construction costs on a first cost basis as long as no provisions are made for increased durability and reduced maintenance and with it for overall reduced life cycle costs. In comparison with conventional structural materials, advanced composites have high material to labor cost ratios which, even with significant efforts in manufacturing automation, can only be reduced final costs nominally.

Recent developments have focused on new hybrid systems which combine the advanced composite materials with conventional construction materials such as the concrete filled carbon shell system (CSS) and conceptual design and optimization studies have shown that even on a first cost basis these new bridge systems can be cost competitive with conventional bridge construction. The

developments and application of advanced composites in new composite construction applications in bridge infrastructure retrofit and renewal are discussed in the following.

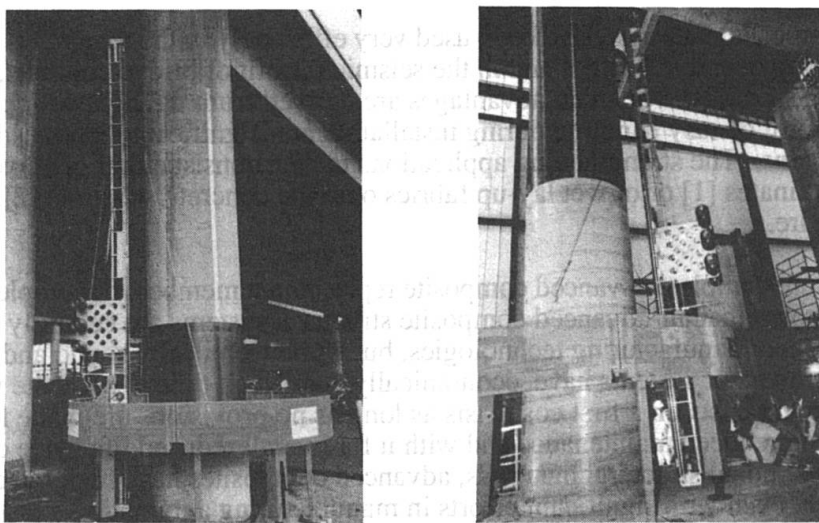
2. Advanced Composites for Bridge Rehabilitation

The rehabilitation of existing bridge structures to eliminate structural deficiencies and to provide extended and increased service capacities can be required in the form of repair of damaged regions, strengthening of substandard components, or retrofit for increased seismic response capacities. In all three areas of rehabilitation, advanced composite materials have been shown to be structurally efficient, easy to install and cost competitive with conventional rehabilitation concepts and procedures, [1, 2].

The addition of advanced composite strips or overlays to existing bridge decks, girders, or columns results in a new composite action which to a large extent depends, in terms of performance characteristics, on the polymer interface between the two materials, on the mechanical characteristics of the substrate, i.e. the surface of the existing material, and on the environmental and time-dependent compatibility of the two materials in terms of chemical interaction, differences in thermal coefficients, and differences in time-dependent effects. The currently practiced "art" of rehabilitation with these new materials needs to be developed into a "science" with established design criteria and guidelines, validated application and quality assurance procedures, and a properly designed and implemented instrumentation and monitoring program to provide the to date uncertain long-term performance and durability characteristics.

At the University of California, San Diego (UCSD) comprehensive research efforts since 1993 [2, 3] into the use of advanced composite rehabilitation concepts for existing structural concrete systems have resulted in (1) strengthening concepts for bridge decks and superstructures with carbon fabric overlays for increased load capacities, (2) strengthening and retrofitting of pier walls with carbon overlays for increased lateral in-plane and out of plane force and deformation capacities, and (3) seismic retrofit concepts for columns through advanced composite jacketing for increased structural ductility.

For example both full scale laboratory validation tests and field applications for Caltrans (California Department of Transportation) on the I-10 Santa Monica Viaduct in Los Angeles, California, have been successfully completed, see Fig. 1, demonstrating not only the technical soundness of the new composite structure under extreme loading conditions but also the economical competitiveness with conventional (steel or concrete jacketing) retrofit procedures.



a) Field Application

b) Full Scale Laboratory Testing

Fig. 1 Seismic Retrofit Application and Validation of a Continuous Carbon Fiber Jacketing System for Two Column Bent on the Santa Monica Viaduct

For the advanced composite retrofit of structural concrete columns, comprehensive design guidelines for (1) shear strengthening, (2) flexural plastic hinge confinement and column bar buckling restraints, and (3) reinforcement lap splice debonding have been developed [3], as summarized in Table 1, which shows the controlling proportionality relationships based on column dimension D in the loading direction and the mechanical characteristics of the advanced composite jacket system in the form of f_{ju} ultimate jacket capacity, ϵ_{ju} ultimate jacket strain and E_j jacket modulus in the hoop direction.

Table 1 Summary of Advanced Composite Jacket Thickness Relationships for Seismic Retrofit

Response Limit State	Shear Strength Enhancement	Plastic Hinge Confinement	Lap Splice Clamping
Composite Jacket Thickness t_j	$t_j \sim \frac{1}{D \cdot E_j} \cdot C_v$	$t_j \sim \frac{D}{f_{uj} \epsilon_{uj}} \cdot C_c$	$t_j \sim \frac{D}{E_j} \cdot C_l$









In Table 1, C_v , C_c and C_l are design values based on relationships developed in [3, 4] for the specific column geometry and seismic demand.

3. Bridge Deck Replacement

Compelling arguments can be made for modular bridge deck replacement systems which are (1) quick and easy to install to minimize traffic interruptions, (2) lighter than conventional concrete decks to provide increased traffic load capacities and/or reduced seismic mass, and provide (3) increased durability, reduced maintenance and longer life cycles.

In a joint research program between DARPA (Defense Advanced Projects Research Agency) and FHWA (Federal Highway administration) modular advanced composites replacement bridge decks with different cores and geometries were developed and tested at UCSD, see test matrix in Table 2.

Table 2 Advanced Composite Replacement Bridge Deck Test Matrix

Configuration								
Manufacturer	Dupont	Dupont	Dupont	Dupont	Lockheed-Martin	Lockheed-Martin	Core-Kraft	Northrop-Grumman
Core L x W	Balsa	Foam Filled Boxes	Foam Filled Truss	Foam Filled Hat	Pultruded Profiles with Face Sheets	Trapezoidal Profiles with Face Sheets	Corrugated Core with Face Sheets	Egg Crate Core
Sub-Component Shear 1m x 0.6m	●	●	●		●			
Sub-Component Flexure 2.4m x 0.6m			●		●		●	
Full Size Double Bending 4.3m x 0.6m		●	●	●	●			●
Prototype Panel 4.6m x 2.3m			●	●		●		

Note: Panel Depth $D = 230$ mm for all Test Specimens

The large and full scale tests to date have shown that advanced composite replacement bridge decks can be manufactured at prototype scale and (1) exhibit a design stiffness between the cracked and uncracked stiffness of a reinforced concrete deck panel, (2) have strengths which exceed those of an equivalent reinforced concrete panel by factors of 4 and more, (3) weigh 1/5 or less of the weight of a concrete panel with the same depth, and (4) costs approximately 3 to 4 times the initial cost of a cast-in-place concrete deck. However, no design optimization has been performed on these panels since the primary objective to date was the manufacturability of full scale bridge deck sections based on different structural cores and manufacturing procedures. Wear and durability tests of advanced composite replacement deck panels are currently in progress in a roadway test section exposed to regular traffic at UCSD.

4. New Bridge Systems

Research and developments to date on the use of advanced composites in civil engineering construction have shown that cost competitiveness with conventional structural materials and construction concepts is difficult to achieve with all-advanced composite structural systems due to the high materials cost contribution. However, developments of new structural concept and systems which combine the superior mechanical and chemical characteristics of strength in tension in the direction of the composite fibers with dominant characteristics of conventional materials such as compression in concrete to form a new type of composite structural system with great technical and economic potential.

One such concept is that of a carbon or carbon/glass hybrid shell system for bridge columns, wherein the use of prefabricated (filament wound) advanced composite tubes serve the dual purpose of formwork for the concrete and reinforcement, see Fig. 2. The composite tubes feature a ribbed inner surface for mechanical interlock with the infill concrete.

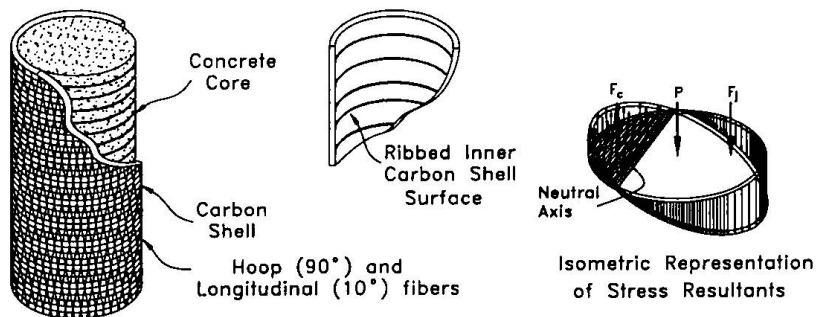
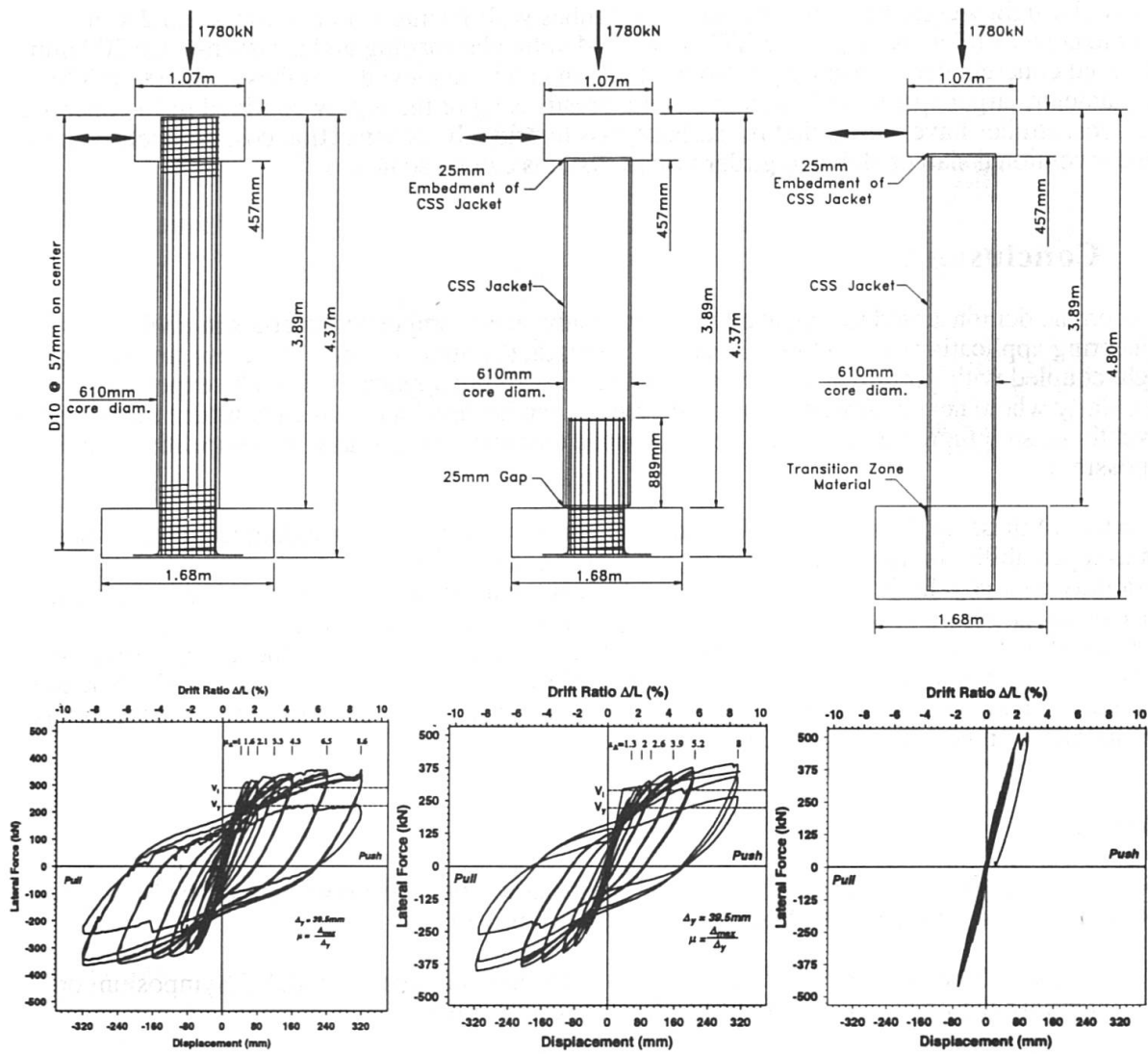


Fig. 2 Concrete Filled Composite Shell Concept

The concrete filled composite shell system replaces conventional reinforcing steel and formwork while providing better confinement to the concrete core, increased durability and greatly enhanced ease of handling and erection speeds. Initial tests on the system comprised of concrete filled carbon shell cantilever columns, see Fig. 3, showed that design objectives of ductile response or elastic strength can be achieved and compared favorably with the corresponding reinforced concrete columns response.

The observed excellent structural response of the concrete filled carbon shell columns [5] allows the development of complete composite bridge systems where concrete filled composite tubes are employed as girders, beams and pylons as outlined in Fig. 4 on the conceptual design of a new composite cable stayed bridge [6].

Leading up to a complete advanced composite cable stayed bridge, as shown in Fig. 4, simple and continuous modular concrete filled composite girder bridge systems are currently under development in a joint research effort with Caltrans and the Federal Highway Administration.



a) Conventional RC Column b) Ductile Design Concept c) Strength Design Concept
 Fig. 3 Concrete Filled Shell Column Tests

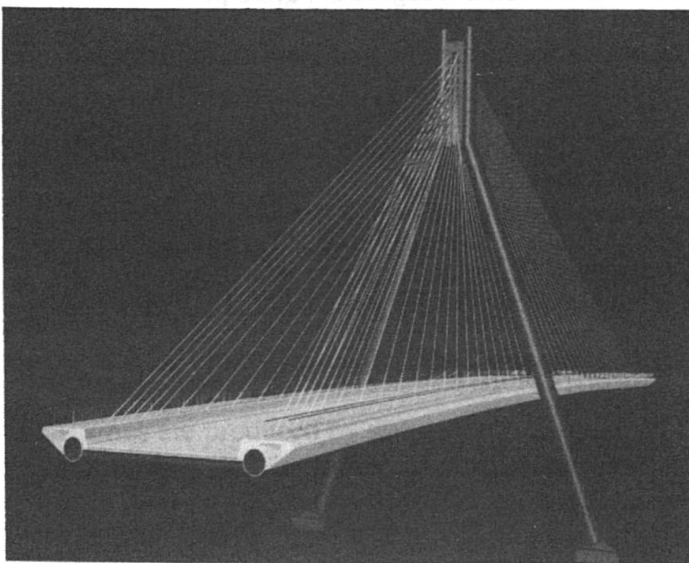


Fig. 4 Advanced Composite Cable Stayed Bridge System

For circular light weight concrete grouted hybrid tubes with 10 mm wall thickness and 2.4 m center to center girder spacing, AASHTO HS-20/44 vehicular loading and a cast-in-place 200 mm reinforced concrete deck, span ranges from 8 to 25 m can be achieved for tubes with 300 to 800 mm diameter, larger spans can be achieved with prestressing of the highly confined infill concrete. Initial cost studies have shown that for carbon/glass hybrid tube construction cost-competitiveness with conventional slab or slab and girder bridge systems can be achieved.

5. Conclusions

Based on the demonstrated technical advantages of advanced composite materials in civil engineering applications of (1) high directional strength, (2) high chemical inertness, and (3) light weight coupled with simplified construction, expanding future applications can be expected. Particularly where new composite structural systems can be developed which combine inexpensive conventional structural materials with new advanced composite materials cost competitive solutions are possible.

The extent of these applications will depend on (1) the resolution of outstanding technical issues such as repeatability in large component manufacturing, durability in the civil environment, reparability and recyclability, (2) the extent to which automation in the manufacturing process can reduce costs, and (3) the availability of validated codes, standards and design guidelines. However, already the worldwide applications to date in bridge repair, strengthening and seismic retrofit, have shown that advanced composites provide viable alternatives for bridge infrastructure rehabilitation and extensions to new composite structural systems for complete bridge replacement or infrastructure renewal are imminent.

References

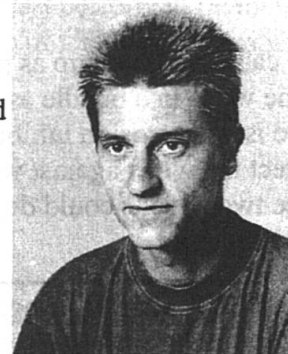
- [1] Meier, U., "Strengthening of Structures Using Carbon Fiber/Epoxy Composites," *Construction and Building Materials*, Vol. 9, No. 6, 1995.
- [2] Seible, F., "Structural Rehabilitation with Advanced Composites," IABSE Symposium on Extending the Lifespan of Structures, San Francisco, 1995.
- [3] Seible, F., Priestley, M.J.N., and Innamorato, D., "Earthquake Retrofit of Bridge Columns with Continuous Carbon Fiber Jackets - Volume II, Design Guidelines" Advanced Composite Technology Transfer Report No. ACTT-95/08, August 1995, 96 pp.
- [4] Priestley, M.J.N., Seible, F., and Calvi, G.M., "Seismic Design and Retrofit of Bridges," John Wiley & Sons, 1996, 686 pp.
- [5] Seible, F., "Design of Structures with Advanced Composites for the 21st Century," IASS Symposium on Conceptual Design, Stuttgart, October 1996.
- [6] Seible, F., Hegemier, G., Karbhari, V., Mertz, D., and Sauvageut, G., "Design Study of an All Advanced Composite Cable Stayed Bridge — I-5/Gilman Bridge in San Diego, Vol. III-Design Criteria," Advanced Composite Technology Transfer Report No. ACTT-96/05, May 1996

Evolution of Stay Cables through the Use of CFRP

Urs MEIER
Prof., Dir.
EMPA
Dübendorf, Switzerland



Heinz MEIER
R & D Eng.
EMPA
Dübendorf, Switzerland



Summary

The excellent properties of the parallel wire bundles made of carbon fiber reinforced polymers (CFRP) include corrosion resistance, very high specific strength and equivalent modulus and outstanding fatigue behavior. The key problem facing the application of CFRP cables and thus their widespread use in the future is how to anchor them. A new reliable anchoring scheme produced with gradient materials based upon ceramics and epoxy and its application on a vehicular cable stayed bridge is described.

Introduction

During the past 20 years, the bridge engineering community has experienced more and more damage on stay and suspender cables. Cables are suffering due to increased corrosion and fatigue loading. Most bridge engineers seem to agree that the corrosion and fatigue resistance of such cables has to be enhanced. The introduction of carbon fiber reinforced polymers (CFRP) instead of steel has been proposed since the early eighties [1]. From the lifetime point of view studies indicated superior results for carbon fiber composites compared to aramid or glass. It was found that the future potential of carbon fibers is highest [2].

CFRP Cables

There are commercial carbon fibers available with elastic moduli ranging from 230 to 650 GPa and strengths from 3500 to 7000 MPa. The elongation at failure varies between 0.6 and 2.4 %. The fiber mostly used within this study and for the bridge in Winterthur was the Torayca T 700S having a strength of 4900 MPa, an elastic modulus of 230 GPa and an elongation at failure of 2.1%. The density is 1.8 g/cm³. The axial thermal expansion coefficient is approximately zero.

CFRP wires are produced by pultrusion, a process for the continuous extrusion of reinforced polymer profiles. Rovings (strands of reinforcement) are drawn (pulled) through an impregnating tank with epoxy resin, the forming die, and finally a curing area. The fibers have a good parallel

alignment and are continuous. The fiber volume content of the wires used in this study was in the range of 65 to 70%. The axial properties of a CFRP wire (modulus, strength) can simply be calculated with the rule of mixture. Measured properties are listed in Table 1. The wires used in this project have diameters of 5 or 6 mm.

The cables are built up as parallel wire bundles. The principal objectives are minimal strength loss of the wires in a bundle as compared to single wires. Since CFRP wires are corrosion resistant there is no corrosion inhibiting compound or grout required. However, it is still necessary to protect the wires against wind erosion and ultraviolet radiation attacks because the combination of these two attacks could degrade the wires. A poly-tetra-fluoroethylene sheath would be adequate for shielding.

Tensile strength σ_{11} (longitudinal)	3300	MPa
Elastic modulus E (longitudinal)	165	GPa
Density	1.56	g/cm^3
Fiber content	68	Vol-%
Thermal expansion (longitudinal)	0.2×10^{-6}	$m/m/^\circ C$

Table 1: Properties of wires pultruded of T700S fibers

The Anchorage of CFRP Cables

The key problem facing the application of CFRP cables and thus the impediment to their widespread use in the future is how to anchor them. The outstanding mechanical properties of CFRP wires mentioned above are only valid in a longitudinal direction. The lateral properties including interlaminar shear are relatively poor. This makes it very difficult to anchor CFRP wire. The evaluation of the casting material to fill the space between the metallic cone of the termination and the CFRP wires was the key to the problem. This casting material, also called load transfer media (LTM) has to satisfy multiple requirements:

- The load should be transferred without reduction of the high long time static and fatigue strength of the CFRP wires due to the connection.
- Galvanic corrosion between the CFRP wires and the metal cone of the termination must be avoided. It would harm the metal cone. Therefore the LTM must be an electrical insulator.

The conical shape inside the socket (Fig. 1a) provides the necessary radial pressure to increase the interlaminar shear strength of the CFRP wires. If the LTM over the whole length of the socket is a highly filled epoxy resin there will be a high shear stress concentration at the loadside of the termination on the surface of the CFRP wire. This peak causes pullout or tensile failure far below the strength of the CFRP wire. We could avoid this shear peak by the use of unfilled resin. However this would cause creep and an early stress-rupture. The best design is a gradient material. At the loadside of the termination the modulus of elasticity is low and continuously increases until reaching a maximum. This way a shear peak can be avoided. The LTM is composed of aluminum oxide ceramic (Al_2O_3) granules with a typical diameter of 2 millimeters (Fig. 1b). All granules have the same size. To get a low modulus of the LTM, the granules are coated with a thick layer of epoxy resin and cured before application. Hence shrinkage can be avoided later in the socket. To obtain a medium modulus the granules are coated with a thin layer. To reach a high modulus, the granules are filled into the socket without any coating. With this method the modulus of the LTM can be designed tailor-made. The holes between the granules are filled by vacuum-assisted resin transfer molding with epoxy resin.

The termination of a 19-wire-bundle is shown in Fig. 1a. Many such bundles were tested at EMPA in static and fatigue loading. The results prove that the anchorage system described is very reliable. The static load carrying capacity generally reaches 92% of the sum of the single wires. This result is very close to the theoretically determined capacity of 94% [3]. Fatigue tests performed on the above described 19-wire cables at EMPA showed the superior performance of CFRP under cyclic loads [2]. The anchorage system is patented worldwide.

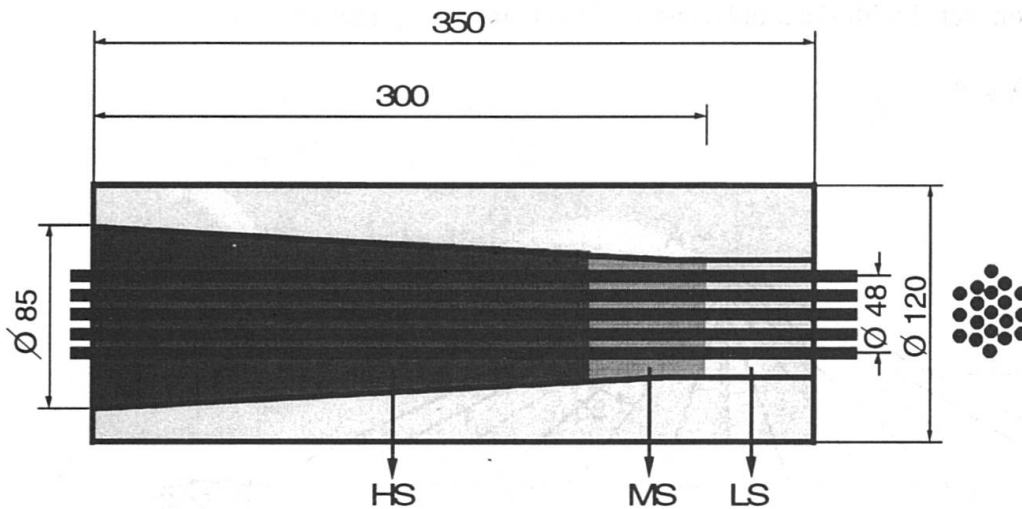


Figure 1a: Conical resin-cast termination; HS=high stiffness, MS=medium stiffness, LS=low stiffness; right side=loadside

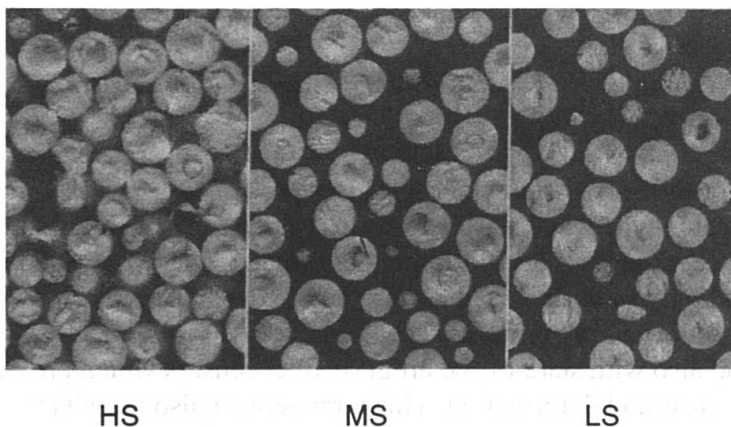


Figure 1b: The load transfer media (LTM) is composed of aluminum oxide ceramic (Al_2O_3) granules with a typical diameter of 2 millimeters; HS=high stiffness, MS=medium stiffness, LS=low stiffness; right side=loadside

The Stork Bridge

The Storchenbrücke, erected in 1996, is situated over the tracks of the railroad station in Winterthur and has a central A-frame tower supporting two approximately equal spans of 63 and 61 meters (Fig. 2). The cables converge at the tower top and are rigidly anchored into a box anchorage at the apex of the A-frame. The superstructure has two principal longitudinal girders (HEM 550, Fe E 460) spaced at 8 m and supporting a reinforced concrete slab. At the anchorage points of the stay cables there are cross girders (IPE 550, E 355). Longitudinal girders and concrete slabs are connected with shear bolts and work as composite girder system.

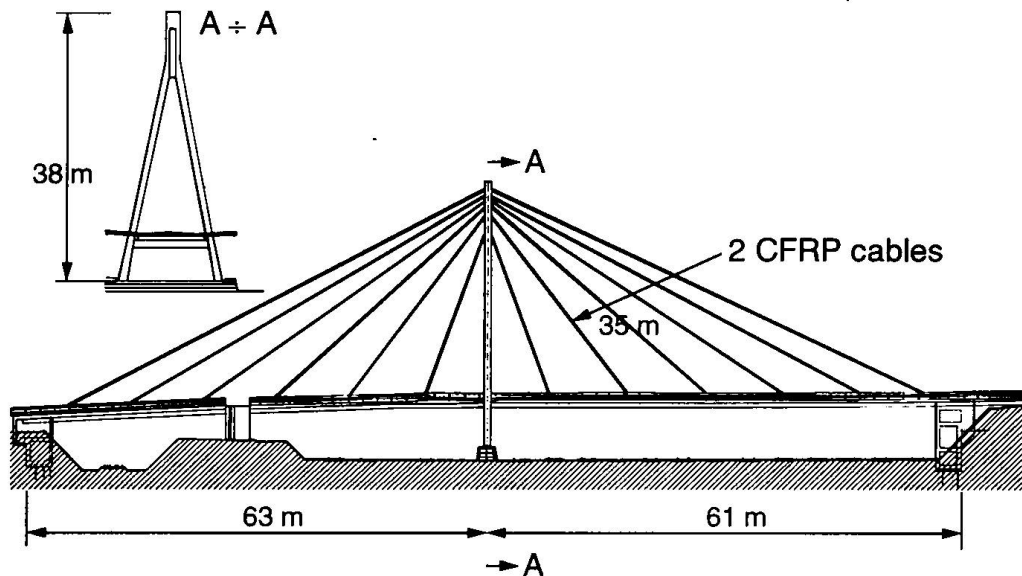


Figure 2: The Storchenbrücke is crossing 14 tracks over the railroad station in Winterthur, Switzerland.

Bridge owner: Town of Winterthur

Design: Höltschi & Schurter, Zürich,

Design and production of the CFRP cables: EMPA Dübendorf and BBR Ltd., Zürich,

Installation of the cables: StahlTon Ltd., Zürich.

The CFRP cable type (Fig. 3) used for the Storchenbrücke (Stork Bridge) consists of 241 wires each with a diameter of 5 mm. This cable type was subjected to a load three times greater than the permissible load of the Storchenbrücke for more than 10 million load cycles. This corresponds to a load several times greater than that which can be expected during the life cycle of the bridge. The 2 CFRP cables with their anchorage and the neighbouring steel cables have been equipped by the EMPA with conventional sensors and also with state-of-the art glass fiber sensors which provide permanent monitoring to detect any stress and deformation. This arrangement also permits a comparison between theoretical modelling and the reality of a practical application.

The cable-stay Storchenbrücke (Fig. 4) will certainly be a milestone in international bridge construction, because CFRP cables do not simply have excellent behavior with regard to corrosion and fatigue but are also five times lighter than steel cables but with the same strength properties. This high strength with low weight will permit us to build bridges in future with considerably longer spans than are currently possible [4, 5].

Conclusions

Suspenders in suspension bridges are regularly replaced throughout the world. Stay cables caused very high maintenance costs in the past 20 years. Many such cables are in need of replacement. There is no doubt that from the technical standpoint CFRP is today the best suited material for suspenders and stay cables. However, since initial cost is the major and often the only parameter used by bridge owners in decision making, it is very difficult for CFRP to compete against steel. Even if the carbon fiber price would decrease within the next five years to a level of 25 Swiss

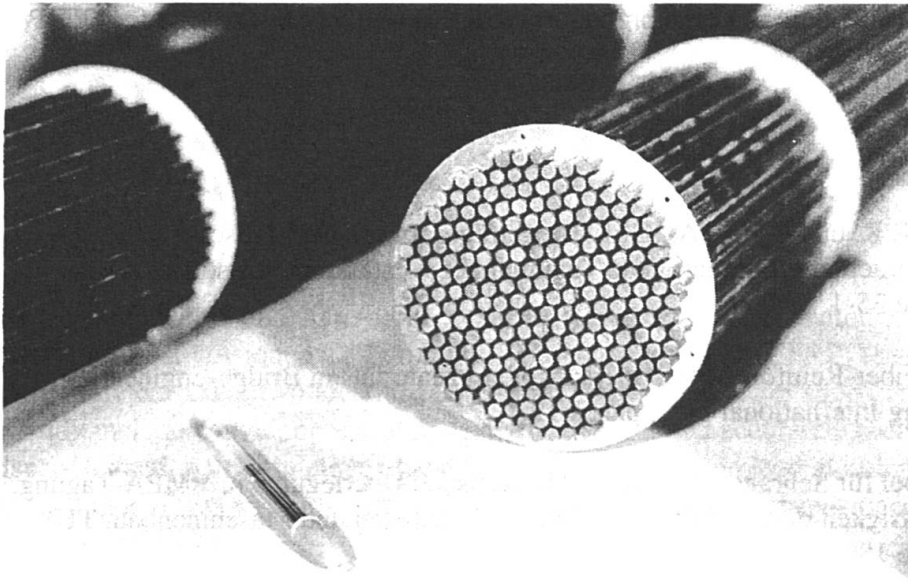


Figure 3: The CFRP cable type used for the Storchenbrücke (Stork Bridge) consists of 241 wires each with a diameter of 5 mm.



Figure 4: The cable-stay Stork bridge may be a milestone in bridge construction.

Francs (18 US \$) per kg (1 kg CFRP is 5.2 times lighter than steel) it will be very difficult for CFRP cables to compete unless the entire life is considered in the costs. A few clients for bridge cables increasingly require worldwide more and more life cycle costing to be carried out. This takes into account the predicted inspection and maintenance costs over the lifetime of the bridge, usually taken as 100 years. Costs are evaluated by calculating the net present value of the expenditure stream using a cash discount rate of typically 6%. CFRP cables benefit considerably compared with steel in such comparisons.

The most important factor to remember is not the cost per kg of materials, but rather the cost effectiveness of the finished product, installed, considering the life expectancy and the costs of the alternatives. This has worked to the advantage of the CFRP sheet bonding technique for rehabilitation of structures and there is a high probability that this will also be the case for CFRP cables in future.

References

- [1] MEIER U., MÜLLER R. und PUCK A., GFK-Biegeträger unter quasistatischer und schwingender Beanspruchung, Internationale Tagung über verstärkte Kunststoffe, AVK Frankfurt, 1982, Seite 35-1.
- [2] MEIER U., Carbon Fiber-Reinforced Polymers: Modern Materials in Bridge Engineering, Structural Engineering International 1/92, pages-12.
- [3] RACKWITZ R., Kabel für Schrägseilbrücken - Theoretische Überlegungen, VMPA-Tagung, Qualität und Zuverlässigkeit durch Materialprüfung im Bauwesen und Maschinenbau, TU München, 1990, Seite 189.
- [4] MENN, CH. and BILLINGTON, D. P., Breaking Barriers of Scale: A Concept for Extremely Long Span Bridges, Structural Engineering International, 1995, pp. 48-50.
- [5] MEIER, U., Proposal for a carbon fibre reinforced composite bridge across the Strait of Gibraltar at its narrowest site, Proc Instn Mech Engrs Vol 201 B2, IMechE 1987, p 73-78

Retrofitting of Prestressed Concrete Beams with Exterior Post-Tensioned CFRP Tendons

Shuaib H. AHMAD
Professor of Civil Engineering
North Carolina State University
Raleigh, NC, USA

Shuaib H. Ahmad is Director of Constructed Facilities Laboratory at North Carolina State University.

Carl V. JERRETT
Research Assistant
North Carolina State University
Raleigh, NC, USA

Carl V. Jerrett received a MS degree from University of Texas, Austin in 1990, and is a PhD candidate at North Carolina State University.

Summary

Tests were conducted on 200 x 400 x 5500 mm steel prestressed concrete beams strengthened with exterior post-tensioned Carbon Fiber Reinforced Polymer (CFRP) tendons. External tendons were harped at two locations and beams were tested under short-term four-point loading. The study included development of an analytical model that accurately predicts the ultimate load, midspan deflection at ultimate load and external CFRP tendon load at ultimate load. The analytical model was used in a parametric study of externally post-tensioned concrete beams.

1. Experimental Program

The experimental program consisted of two "control" prestressed beams and four prestressed beams with external post-tensioned CFRP tendons. The beams were tested to failure. Details are provided elsewhere [1].

1.1 Test Set-up and Procedure

The cross-sectional details of the test beams prior to addition of external tendons are shown in Figure 1. A profile of the test specimens with the CFRP exterior tendons is shown in Figure 2. Steel stirrups of #2 wires were provided as reinforcement in the shear span of the beams, placed at 200 mm spacing, excluding the center 900 mm of the beams. Average concrete strength at time of testing was 44.2 MPa.

For prestressed beams strengthened by external CFRP tendons, one CFRP tendon was placed on each side of the beam. Attachment of the CFRP tendons to the ends of the concrete beam was accomplished using a steel U-shaped device attached to the end of the beams at the midheight of the beam (200 mm from top). Harping of each of the CFRP tendons at the midspan of the beams was provided at two locations spaced 710 mm apart and symmetric about the midspan of the beam. At midspan, the tendons were located a depth of 390 mm from the top of the beam, which was approximately the bottom of the beam. Harping points consisted of aluminum plates cut to a radius of 510 mm, with a semicircular groove cut along the arch with a diameter of 8 mm. The initial harping angle of the tendon at each harping point was 4.8 degrees. The average post-

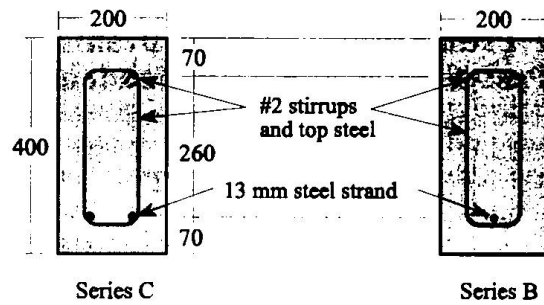


Fig. 1 Cross-section of beam specimens

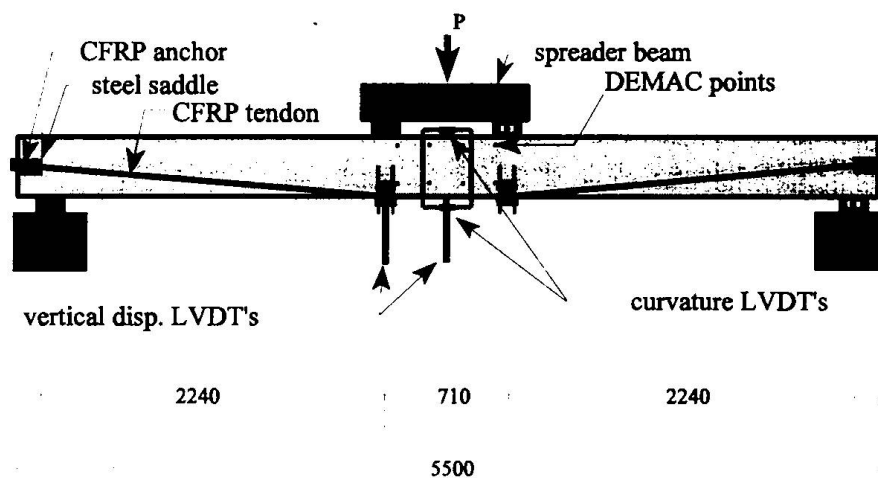


Fig. 2 Schematic diagram of the prestressed beams strengthened by external CFRP tendons

tensioning force per CFRP tendon was 124 kN.

The beam span was 5190 mm with point loads spaced 710 mm apart and symmetric about the midspan of the beam. Vertical deflections of the beams were measured at two locations: midspan of the beams and at one of the two loading points. Strains in the CFRP tendons were measured using surface mounted strain gages.

All tests were conducted under displacement control. Displacements were applied at a rate of approximately 5 mm/minute. To simulate damaged beams in service, all beams were initially loaded to just beyond their cracking load and then unloaded to 19 kN. This initial limit load for the beams was 37 kN and 64 kN for the B series beams and C series beams, respectively. For the control beams, after reducing the load to 19 kN, the load was increased until failure, which was initiated by crushing of the concrete. For the strengthened beams, after reducing the load to 19 kN, the CFRP tendons were post-tensioned. The deflection associated with the 19 kN load was maintained on the beam throughout the post-tensioning process. At the completion of post-tensioning, the vertical load on the beam increased due to the camber affect induced by post-tensioning. The load on the beam was again reduced to 19 kN before loading the beam to failure.

1.2 Test Results

Load-midspan deflection curves for beams B-0, B-1, C-0 and C-1 are shown in Figures 3 and 4. Results for beams B-2 and C-2 were similar to results for B-1 and C-1, respectively. The figures also show the results of the analytical analysis discussed later. A summary of the test results for the beam tests is presented in Table 1. Table 1 does not include results for the analysis including tension stiffening affects (TS analysis).

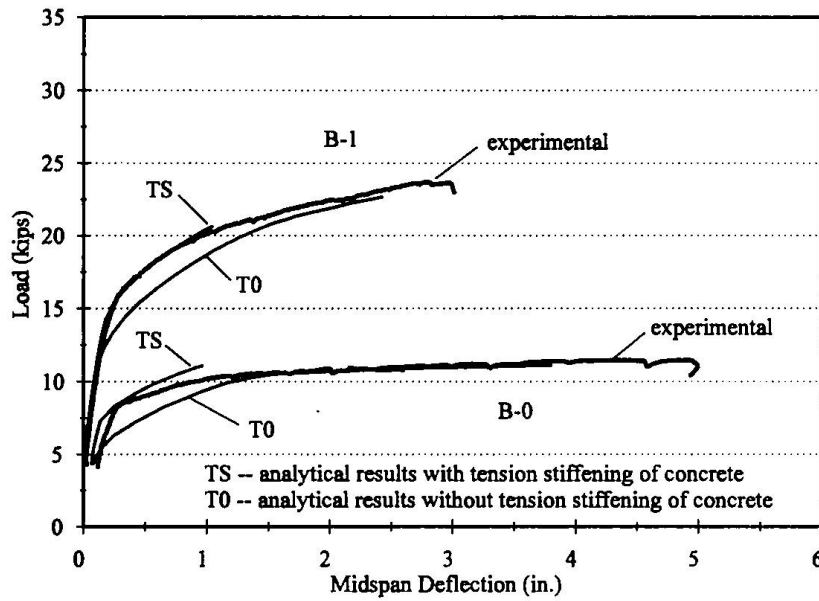


Fig. 3 Experimentally observed and predicted load-midspan deflection for B-0 and B-1

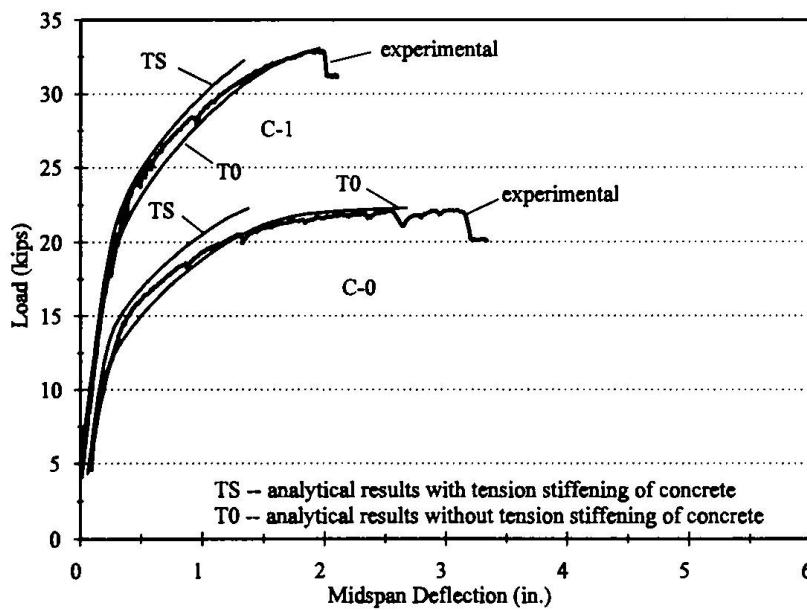


Fig. 4 Experimentally observed and predicted load-midspan deflection for C-0 and C-1

Table 1 Summary of experimental and analytical beam test results

Beam No.	Ultimate load, kN		Midspan deflection at ultimate load, mm		Initial total force of external CFRP tendons, kN	Total force of external CFRP tendons at ultimate, kN	
	Exp.	Analytical	Exp.	Analytical		Exp.	Analytical
B-0	51.2	49.4 (0.97)	113	96.8 (0.86)	--	--	--
B-1	105	101 (0.96)	71.4	61.7 (0.86)	117	169	164 (0.97)
B-2	108	103 (0.95)	68.8	57.9 (0.84)	127	179	171 (0.96)
C-0	98.7	99.2 (1.00)	78.5	68.1 (0.87)	--	--	--
C-1	147	147 (1.00)	50.5	50.0 (0.99)	128	164	164 (1.00)
C-2	147	145 (0.99)	50.5	49.5 (0.98)	124	161	158 (0.98)

() numbers in parenthesis indicate the percent (%) of experimental value

Failure of the beams for all tests was due to crushing of concrete at the top of the beam. Ultimate loads for beams post-tensioned with external CFRP tendons averaged 55 and 48 kN higher than their companion non-post-tensioned beams (Table 1). This corresponds to an ultimate strength of 209% and 149% of the companion non-post-tensioned beam strength for the B series and C series beams, respectively. Midspan deflections at ultimate for the externally post-tensioned beams averaged approximately 64% of the midspan deflection at ultimate for the companion non-post-tensioned beams for both B and C series beams.

As shown in Figures 3 and 4, the exterior post-tensioned beams had a positive tangential stiffness, defined as the change in load divided by the associated change in midspan deflection, up to failure. This was not evident for the non-post-tensioned beams B-0 and C-0. It was found in more detailed analysis that this positive tangential stiffness at failure was due to the increased upward forces at the harping points. The increased upward forces at the harping points was due to the beam deflections which caused larger bend angles of the tendons at the harping points and caused increased forces in the external tendons due to additional strains in the tendons.

Figure 5 shows the variation in total external CFRP tendon force with the midspan deflection. It is evident in the figure that the external CFRP tendon strains, and therefore tendon forces, varied linearly with the midspan deflection of the beams. The response for beams C-1 and C-2 varied in a similar manner. The external CFRP tendon forces at ultimate averaged 143% and 129% of the initial external CFRP tendon forces for the B series and C series beams, respectively (Table 1).

2. Analytical Model

As part of this study, a computerized analytical model was developed that accurately predicts the ultimate load, midspan deflection and external tendon force at ultimate for externally post-tensioned, simply supported beams loaded symmetrically about the midspan with two point

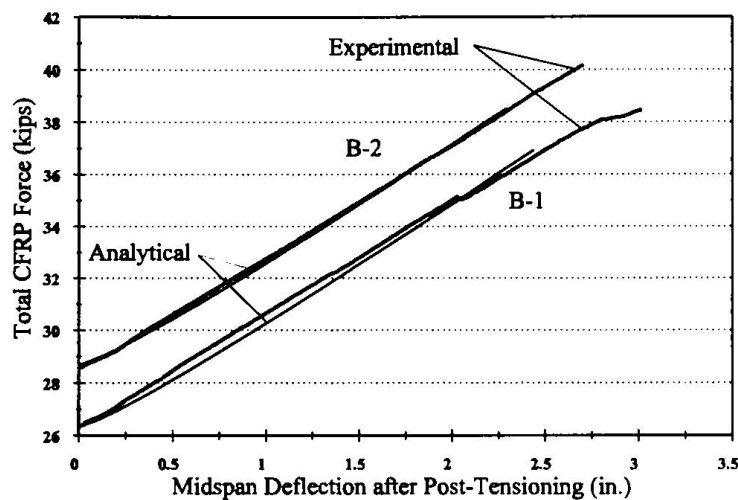


Fig. 5 Total CFRP tendon force versus midspan deflection after post-tensioning, B-1 and B-2

loads. External tendons are harped at two locations symmetric about the midspan of the beam and no friction is assumed at the harping points of the tendons. The analytical model was included in a computer program called EXPOST.

2.1 Development of Analytical Model

The analytical model uses a constitutive relationship for concrete developed by Ahmad [2]. Constitutive relationship for the prestressing steel was modelled as linear up to yielding, represented by a fourth-order polynomial expression at yielding, and then linear prior to reaching ultimate strain. Non-prestressed steel reinforcement was model as linear up to yielding with no strain hardening. CFRP tendons were modelled as linearly elastic.

At each load increment, the model assumes an external CFRP tendon force and determines beam segment curvatures. Curvatures are integrated over the span length to determine displacements. After displacements are determined, a CFRP tendon force is predicted using the initial CFRP tendon force plus additional forces due to straining of the external tendons resulting from vertical displacements at the harping points and horizontal extension of the beam at the height of the tendon anchorage. If the predicted and assumed CFRP tendon forces are within 0.05%, then the beam load is increased to the next load level, otherwise, the analysis is repeated with a new assumed CFRP tendon force. If the predicted and assumed CFRP tendon forces are within a tolerance (assumed to be 0.05%) and the maximum load on the beam is greater than the maximum allowable load of a beam section, the beam is considered to have failed.

2.2 Comparison Between Analytical and Experimental Results

As shown in Figures 3, 4 and 5 and in Table 1, the computerized analytical model developed in this study accurately predicts the ultimate load, ultimate midspan deflection and the CFRP tendon force at ultimate for the beams tested as a part of this study. Predictions of ultimate load ranged between 95% and 100% of the experimentally observed ultimate load. Midspan deflections were slightly under predicted (84% to 99% of the experimentally observed deflections). Predictions of the CFRP tendon forces at ultimate ranged between 96% and 100%

of the experimentally observed CFRP tendon forces.

2.3 Results of Parametric Study

The computer program EXPOST was used in a parametric study of steel prestressed concrete beams externally post-tensioned with CFRP tendons. Two types of beams were considered -- rectangular and T-beams, with two amounts of effective prestress force for each type of beam. The dimensions of the rectangular beams were 152 mm x 406 mm and of the T-beams were 51 mm x 610 mm top flange and 356 mm x 102 mm web. The effective prestress force was varied by changing the area of prestressing steel from 77 to 161 sq.-mm for the rectangular beams and from 174 to 374 sq.-mm for the T-beams, with the effective steel prestress remaining 1030 MPa. The depth of prestressing steel for both beams was 330 mm. Span lengths for the beams were 6.1 m and 9.1 m for the rectangular and T-beams, respectively. Variables for the parametric study were the initial total load of the external tendons (53 to 160 kN), the harping point location for the external tendons (either at the midspan or at 1/3 span of the beam), and the axial stiffness of the external CFRP tendons (7120 to 24000 kN/m/m).

Results of the parametric study indicate that the ultimate load of externally post-tensioned beams increases with increases in initial force of the external tendons, harping at third-points versus midpoints of the beam, and with increases in the stiffness of the external tendons. Increases in ultimate loads averaged 172% of the companion non-post-tensioned reference beam ultimate load. Beams with external tendons harped at third-points showed an average increase in ultimate load 15% higher than beams with external tendons harped at midspan. Midspan deflections at ultimate for the beams reduced an average of 46% due to the addition of external post-tensioning.

Increases in the external CFRP tendon forces at ultimate was significant. For the rectangular and T-beams, forces in the external CFRP tendons at ultimate averaged 158% and 205% of the initial tendon forces, respectively. For each of the four types of beams investigated in the study, little difference was observed in the energy absorption capacity of the beams at failure.

3. Summary and Conclusions

Results of this study showed that externally post-tensioned CFRP tendons can be effectively used for strengthening of prestressed concrete beams. The behavior of externally post-tensioned prestressed beams can be predicted using the computerized model developed in this study.

4. References

1. Jerrett, C. V., "Performance of Carbon Fiber Reinforced Polymer (CFRP) Tendons and their use for Strengthening of Prestressed Concrete Beams," PhD Dissertation, North Carolina State University, 1996.
2. Ahmad, S. H., "Strength and Ductility of Prestressed Concrete Beam-Column Elements Using High Strength Concrete," Proceedings, International Symposium on Concrete in Developing Countries, Jan 1986, pp. 707-129.

Concrete-Filled Fibre Reinforced Plastic Circular Columns

Duncan LILLISTONE

Research Assistant
University of Southampton
Southampton, United Kingdom

Duncan Lillistone graduated from the University of Southampton in 1994. After a period working on bridge assessments, he has been researching composite columns at the University.

Colin K. JOLLY

Head of Structures Research Group
University of Southampton
Southampton, United Kingdom

On graduation Colin Jolly spent five years designing water-retaining and building structures in the UK and Oman. In his postgraduate degrees and subsequent research he has developed a wide range of cementitious composites and their design methodologies.

Summary

An experimental investigation was conducted to determine the strength enhancement of concrete columns due to confinement provided by filament wound glass fibre tubes used as permanent formwork. The principal variables were concrete strength, slenderness and angle of fibre alignment. Significant increases in compressive strength were achieved. A design approach has been proposed which uses existing design equations, modified to reflect the increased confidence in the effective compressive strength of concrete.

1. Introduction

Research has shown that Fibre-Reinforced Plastics (FRP) reinforcement can successfully be used as the tensile component to reinforce concrete beams in bending [1]. However, their use as longitudinal reinforcement in compression members is not economic due to the relatively low compressive modulus and strength of FRP composites [2]. The purpose of the research described in this paper is to investigate the use of FRP composites as confinement reinforcement for concrete. Experimental work into the behaviour of confined concrete has shown that there is a significant increase in both strength and ductility of the concrete. This form of construction offers additional advantages since the FRP composite serves as permanent formwork and provides a barrier against aggressive agents, thus improving the column's durability. Using the FRP composite as peripheral reinforcement for circular columns results in the FRP composite acting in direct tension to develop the confining hoop stress.

Previous researchers have examined the enhanced properties of concrete cylinders confined by FRP composite wraps, and a number of empirical design equations have been proposed [3-5]. These design equations are based on experimental work using small specimens and the results cannot be taken as representative of the behaviour of realistically sized columns. To investigate the behaviour of full scale concrete columns confined with FRP composites, an extensive test programme is being under taken at the University of Southampton. Additionally, ten large diameter columns were tested in collaboration with the Building Research Establishment. The preliminary results of part of this test programme are presented in this paper.

2. Experimental Programme

2.1 Materials

2.1.1 Concrete

One of the primary objectives of the test programme is to investigate the influence of concrete strength. Two different concrete mixes were designed to have compressive cube strengths of 25 N/mm² and 35 N/mm². All the tubes were cast in the vertical position as would normally be the case in construction. The concrete was dropped into the tube from the top, and vibrated internally by a poker vibrator. To minimise segregation of the concrete, a cohesive concrete was used with a slump of 50mm.

2.1.2 Filament Wound Tubes

The filament wound tubes were supplied by Fibaflo Plastic Ltd. The tubes consist of 51% continuous E-glass fibres by volume, embedded in an epoxy resin. The tensile strength of the basic E-glass fibre is 3400 N/mm² with an elongation of 4.5% at failure [6]. Three different nominal angles of fibre alignment were tested; 90°, 67.5° and 45°, the angle of fibre alignment being measured from the longitudinal axis. Limitations imposed by the filament winding machinery meant that the actual winding angles differed from the nominal values. The properties of the tubes are shown in Table 1. The theoretical confining pressure is given by Equation 1:

$$f_{lat} = \frac{2t}{D} v_f \sigma_f \sin^2 \alpha \quad \text{Equation 1}$$

Diameter ϕ mm	Standard Deviation mm	Thickness t mm	Standard Deviation mm	Fibre Alignment α degrees	Confining Pressure f_{lat} N/mm ²
59.86	0.21	2.53	0.14	75.5	137.38
79.85	0.09	2.46	0.11	78.1	102.30
79.89	0.04	2.48	0.11	57.8	77.08
79.89	0.07	2.66	0.15	43.4	54.51
99.97	0.09	2.45	0.13	80.4	82.63
100.02	0.10	2.28	0.14	71.4	71.01
100.03	0.05	2.22	0.10	49.9	45.03
300.10	0.09	3.80	0.11	86.8	43.78
399.88	0.21	5.07	0.09	87.6	43.89

Table 1 Dimensions of filament wound tubes

2.2 Experimental Procedure

Tests at the University of Southampton were carried out on either a 2000 kN Losenhausen or 1500 kN Instron column rig. Both machines were operated in position-control for safety reasons due to the brittle failure mechanism of the specimens. The additional tests at the BRE were carried out on their 10000 kN load-controlled Amsler column rig.

2.2.1 Axially Loaded Columns

The columns were tested in axial compression to failure. Measurements consisted of load, crosshead displacement, axial and circumferential strain. Axial strains were measured over the middle half of their length using an extensometer, consisting of four LVDT's positioned at four orthogonal points. The extensometer was removed at an axial strain of 2% to prevent damage to the instrumentation and to eliminate any additional confinement induced by the extensometer. The

circumferential expansion of the cylinders was determined by an LVDT attached to the end of a sheathed cable positioned at mid-height around the periphery of the cylinder.

The columns were loaded in equal displacement increments of 0.001 mm/min/ mm length of sample. Readings were taken automatically using an Amplicon PC226 data acquisition board in a Pentium PC. To minimise errors due to fluctuations in the electrical supply, a filtered power supply was used and each reading consisted of an average 1000 samples taken over one second.

2.2.2 Eccentrically Loaded Columns

Two column lengths were investigated with length/diameter ratios of 5 and 10. The columns were tested to failure under eccentric compression. All loading was of short duration; the effects of sustained or repeated loading were not investigated. Measurements consisted of load, crosshead displacement, lateral deflection at mid and quarter heights, and both axial and circumferential strains. The eccentricity of all the columns was 5% of the internal diameter. The load was applied by increasing the platen displacement in equal increments determined from the cylinder tests. Each test to failure lasted approximately 50 minutes.

3. Experimental Results and Discussion

3.1 Axially Loaded Columns

Table 2 gives the strength and deformation at failure for the confined columns. The strength clearly increases as the orientation of the fibres approaches the hoop direction. Figure 1 shows the stress-strain curve for the 80mm diameter specimens. The shape of the curves is initially similar to plain concrete, and once the unconfined concrete strength is exceeded the curve continues in a linear manner with a reduced slope. The stiffness of the secondary slope is a function of the orientation of the fibres, with the stiffness increasing as the fibres angle of wind approaches the hoop direction. Ultimate failure was achieved for all the specimens except fw112 and fw113. However, creep failure of specimen fw112 was achieved under a sustained load of 10140 kN for 6 minutes.

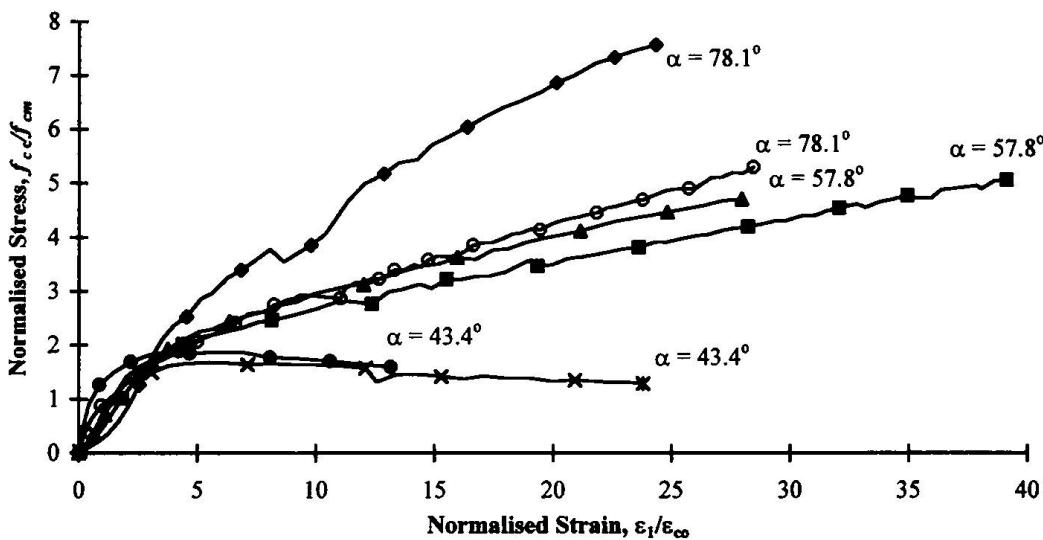


Fig 1 Stress- Strain Relationship for Axially Load Columns

The orientation of the fibres was also found to influence the failure mechanism of the cylinders. Cylinders where the fibres are aligned at angles close to the hoop direction failed by fibres rupturing then unwrapping about the middle third of the specimen. Fibre orientation of approximately 67.5° caused a tensile rupture of the fibres along the entire length of the cylinder. Cylinders with fibres at approximately 45° , resulted in a compressive failure mode of the fibres.

The measured circumferential strains are significantly less than the theoretical rupture strain of the basic fibre. This corresponds with observations during testing where the large axial deformations resulted in premature tensile failure of the fibres, due to localised compression. Consequently, the theoretical confining pressure of the fibres is not achieved, with an increasing reduction as the winding angle reduced.

The degree of compressive strength enhancement is a function of both the confining pressure and unconfined strength of concrete. It was found that the lower strength concrete exhibited a greater increase in compressive strength and ductility. In general, lower strength concrete is more ductile and the proportionately greater lateral expansion results in larger confining pressures.

Ref. No.	Diameter ϕ mm	Fibre Alignment	Failure Load kN	Failure Stress, f_{cc} N/mm ²	f_{cc}/f_{cu}	Axial Strain %	Circumferential Strain %
fw1	59.86	75.5	445.4	158.3	7.40	4.46	-1.25
fw2	59.86	75.5	416.2	147.9	5.44	4.05	-1.16
fw7	79.85	78.1	888.6	177.4	7.57	4.87	-1.63
fw8	79.85	78.1	934.3	186.6	5.30	5.70	-1.57
fw15	79.89	57.8	572.1	114.1	5.06	7.83	-4.98
fw16	79.89	57.8	775.1	154.6	4.71	5.60	-3.08
fw23	79.89	43.4	248.9	49.7	1.68	1.90	-1.21
fw24	79.89	43.4	234.0	46.7	1.49	1.14	-1.47
fw31	99.97	80.4	973.1	124.0	6.30	3.78	-1.29
fw32	99.97	80.4	1129.4	143.9	3.95	3.17	-1.23
fw39	100.02	71.4	913.9	116.3	4.13	5.41	-3.42
fw40	100.02	71.4	820.7	104.5	4.08	2.02	-3.37
fw47	100.03	49.9	458.5	58.3	1.87	-	-
fw48	100.03	49.9	414.9	52.8	2.14	-	-
fw107	300.10	86.8	5980	84.5	3.49	2.58	-1.40
fw108	300.10	86.8	6050	85.5	2.46	2.13	-1.32
fw112	399.88	87.6	10140	80.7	3.27	2.41	-1.15
fw113	399.88	87.6	9750	77.6	2.13	1.94	-0.97

Table 2 Limiting Strength of Axially Loaded Columns

3.2 Eccentrically Loaded Columns

Figure 2 shows that the ultimate load for concrete columns is significantly increased by the filament wound tube. Greater axial loads and moments are achieved with tubes where the fibres are aligned at an angle between 67.5° and 80.4° . However, large lateral deflections are associated with these enhanced loads and serviceability requirements restrict the degree of enhancement achieved. Table 3 gives the axial loads at a compressive strain of 0.35%, the limiting compressive strain specified in BS8110. Figure 2 shows the failure envelope for plain concrete, based on a limiting compressive strain of 0.35% and a concrete strength of $0.67f_{cu}$. Comparison of the axial load of the columns at a compressive strain of 0.35% still shows an enhancement in the load carrying capacity.

Ref. No.	ϕ mm	α	Length mm	f_{cu} N/mm ²	e mm	Failure Load kN	δ mm	Moment kNm	Readings @ 0.35% Strain		
									Load kN	δ mm	Moment kNm
fw4	59.86	75.5	370.0	27.9	3.0	167.4	9.67	1.62	101.5	3.83	0.39
fw5	59.86	75.5	370.0	36.2	3.0	171.6	10.94	1.88	75.8	3.50	0.27
fw6	59.86	75.5	670.2	32.3	3.0	92.3	11.80	1.09	65.9	5.50	0.36
fw9	79.85	78.1	467.8	19.7	4.0	311.7	15.13	4.72	94.0	4.60	0.43
fw10	79.85	78.1	469.6	36.4	4.0	367.4	-	-	172.2	4.29	0.74
fw12	79.85	78.1	869.7	31.2	4.0	200.5	15.85	3.18	103.7	6.22	0.64
fw13	79.85	78.1	867.9	25.6	4.0	171.0	14.72	2.52	127.8	6.06	0.77
fw17	79.89	57.8	469.6	28.2	4.0	242.8	11.54	2.80	121.6	4.52	0.55
fw18	79.89	57.8	469.1	24.6	4.0	213.0	10.72	2.28	92.3	4.48	0.41
fw20	79.89	57.8	869.0	21.5	4.0	130.9	11.82	1.55	114.7	4.11	0.70
fw21	79.89	57.8	869.7	27.2	4.0	188.2	8.44	1.59	135.5	4.13	0.56
fw25	79.89	43.4	469.1	30.7	4.0	172.3	6.55	1.13	129.5	4.43	0.57
fw26	79.89	43.4	469.9	34.4	4.0	185.1	7.20	1.33	153.0	4.81	0.74
fw29	79.89	43.4	789.9	34.3	4.0	150.0	9.35	1.40	146.2	6.35	0.92
fw33	99.97	80.4	569.7	23.4	5.0	447.3	18.77	8.40	157.9	-	-
fw34	99.97	80.4	569.9	35.2	5.0	568.4	16.98	9.65	231.2	5.11	1.18
fw36	99.97	80.4	1068.9	22.6	5.0	278.3	16.38	4.56	179.0	6.58	1.18
fw37	99.97	80.4	1070.3	32.8	5.0	311.8	15.66	4.88	226.1	6.43	1.45
fw41	100.02	71.4	569.6	29.5	5.0	392.0	16.50	6.47	228.3	5.44	1.24
fw42	100.02	71.4	569.9	31.3	5.0	398.2	14.58	5.81	223.4	5.84	1.30
fw44	100.02	71.4	1069.1	21.4	5.0	188.7	16.69	3.15	168.6	8.42	1.42
fw45	100.02	71.4	1069.8	33.2	5.0	236.8	16.46	3.90	219.3	9.05	1.98
fw49	100.03	49.9	569.9	33.7	5.0	240.2	11.49	2.76	148.3	5.74	0.85
fw50	100.03	49.9	569.9	40.1	5.0	272.8	10.67	2.91	210.6	5.50	1.16
fw52	100.03	49.9	1068.7	30.0	5.0	154.4	13.91	2.15	147.2	9.04	1.33
fw53	100.03	49.9	1069.3	29.3	5.0	176.9	12.91	2.28	171.6	9.88	1.69
fw109	300.10	86.8	1650	25.3	15.0	2530	32.45	82.10	1500	18.25	4.87
fw110	300.10	86.8	1650	36.8	15.0	3300	31.33	103.39	-	-	-
fw111	300.10	86.8	3150	39.7	15.0	2100	26.28	55.19	-	-	-
fw114	399.88	87.6	2150	29.0	20.0	5050	56.44	243.52	-	-	-
fw115	399.88	87.6	2150	40.5	20.0	5860	38.75	227.08	3680	24.89	17.99
fw116	399.88	87.6	4150	36.5	20.0	3300	26.07	86.31	-	-	-

Table 3 Experimental Results of Confined Columns

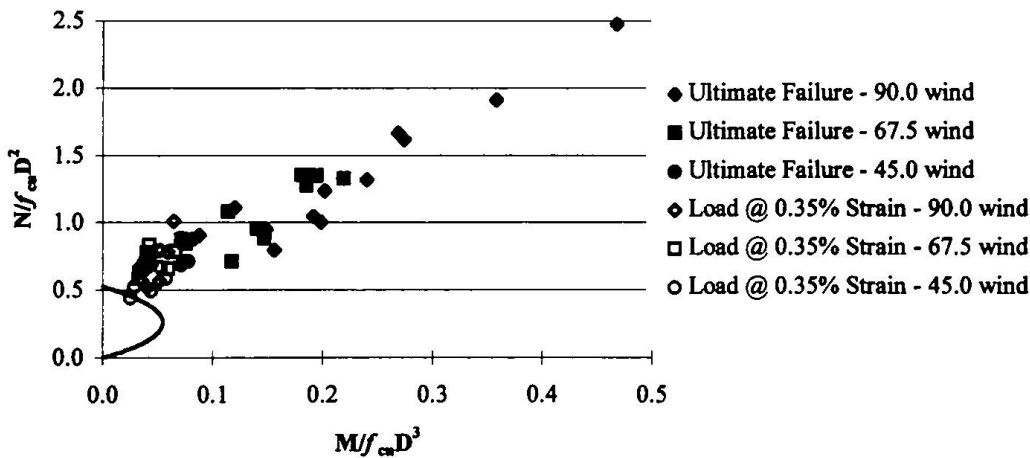


Fig 2 Interaction Diagram for Concrete Filled GFRP Columns

Consequently, the column design equation for stocky columns given in BS8110 [7] can be modified.

$$N = 0.45C_m f_{cu} A_c + 0.87f_y A_{sc} \quad \text{Equation 2}$$

Where C_m is an empirical coefficient that reflects the increased confidence in the strength of the concrete. Based on the preliminary results presented in this paper, the value C_m lies between 1.15 and 1.20. Limiting the concrete compressive strains to a value 0.35% also means that the existing deflection prediction equations are still valid.

4. Conclusion

Preliminary test results have shown than a significant enhancement in axial load carrying capacity can be achieved using glass fibre filament wound tubes as permanent formwork. It is not recommended that design be based on the ultimate limit state of the tube. Since, at ultimate limit state, the concrete is a highly fissured material, any loss of the confining pressure at strains exceeding 0.35% would result in immediate brittle collapse. However, designs based on existing reinforced concrete design codes can be modified to take account of the increased confidence in the strength of plain concrete, using the material confinement factor C_m value between 1.15 and 1.20 obtained statistically from these results.

5. References

1. Clarke, J. L. and Waldron, P. 'The reinforcement of concrete structures with advanced composites', *The Structural Engineer*, Vol. 74, No. 17, 1996, p 283-288.
2. Kobayashi, K. and Fujisaki, T. 'Compressive behaviour of FRP reinforcement in non-prestressed concrete members', *Non-Metallic (FRP) Reinforcement for Concrete Structures* (ed. L. Taerwe), London, E & FN Spon, 1995, p 267-274.
3. Fardis, M. N. and Khalili, H. H. 'FRP-encased concrete as a structural material', *Magazine of Concrete Research*, Vol. 34, No. 121, 1982, p 191-202.
4. Harmon, T. G. and Slattery, K. T. 'Advanced composite Confinement of concrete', *Advanced Composite Materials in Bridges and Structures* (ed. K. W. Neale and P. Labossiere), Canadian Society for Civil Engineering, 1992, p 299-306.
5. Howie, I. and Karbhari, V. M. 'Effect of tow sheet composite wrap architecture on strengthening of concrete due to confinement: I-experimental studies', *Journal of Reinforced Plastics and Composites*, Vol. 14, No. 9, 1995, p 1008-1030.
6. Glass Reinforcement Data Book, VETROTEX (UK) Ltd, Wallingford, 1995.
7. BS8110, *Structural use of Concrete: Part 1: Code of Practice for Design and Construction*, British Standards Institution, London, 1985.

The Design and Development of a Novel FRP Reinforced Bridge

Stein Atle HAUGERUD

Dipl. Ing.
Dr. techn. Olav Olsen a.s.
Oslo, Norway

Born in 1964, S.A. Haugerud obtained his diploma in civil engineering at the Technische Hochschule Darmstadt in 1990. He then joined the company Dr. techn. Olav Olsen a.s. and has since 1992 been section head of Applied Structural Technology.

Lars Lund MATHISEN

B. Eng. (hons)
Dr. techn. Olav Olsen a.s.
Oslo, Norway

L.L. Mathisen, is a graduate from University of Manchester, Institute of Science and Technology, England. Has since 1992 worked in the Structural Engineering company Dr. techn. Olav Olsen a.s, currently in the department of Structural Technology.

Summary

The Oppegaard Trial bridge forms a part of the R&D project Eurocrete, which is a large European research programme, with the objective to develop the use of non-metallic reinforcement in concrete structures. Both ordinary and post tensioned reinforcement is made of non-metallic composite materials, which makes the bridge the first of its kind built in Europe. Erection of the bridge structure demonstrates the possibility of designing and constructing a bridge with solely non-ferrous reinforcement.

1. Introduction

Corrosion of reinforcement represents a permanent threat against reinforced concrete's durability. Renovation of concrete structures is often attended with considerable costs. In Europe, more than 25 % of all concrete bridges are deteriorated due to carbonation or chloride attack, and the annual costs of corrosion are estimated to 700 millions ECU. Substantial resources are therefore utilised to improve the quality of structural concrete. There is however, little doubt that a reinforcement material that does not corrode and can resist aggressive environments would be the simplest solution. Future maintenance costs have become essential to the owner of any structure. Hence the potential for non-ferrous material as a replacement or supplement to conventional steel reinforcement is considerable, particularly for structures in aggressive environment, such as most bridges.

Eurocrete is a 4-year (1994-1997) 2.8 million ECU European research project, with the objective to develop the use of non-ferrous reinforcement in concrete structures. The research programme comprises several full-scale trial structures that will help assessing the behaviour and durability of the reinforcement in a realistic environment. One of these trial structures is a 10 m long service bridge located on a golf course outside Oslo (Fig. 1). The purpose with the field trial is:

- to monitor and assess long-term behaviour of the FRP reinforcement in a realistic environment
- to monitor immediate short term behaviour
- to supplement laboratory tests
- to validate theoretical models and analytical approaches for response predictions
- to demonstrate the possibility of making a steel-free concrete bridge

In order to achieve the objectives with the trial structure, the bridge is equipped with instrumentation that will register deflection and displacements.

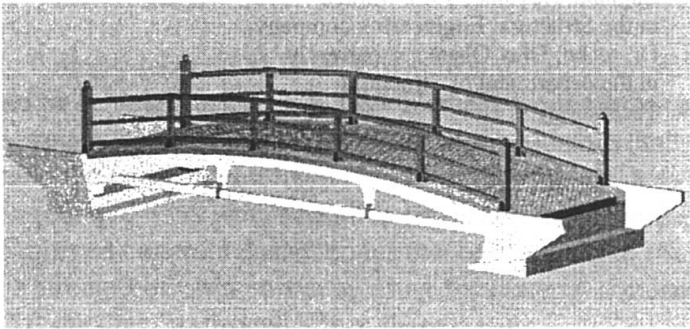


Fig. 1 Rendered image of the golf course service bridge

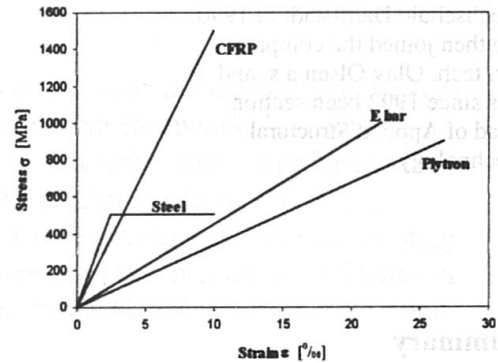


Fig. 2 Stress / strain diagram for FRP materials used

2. FRP Reinforcement

FRP reinforcement consists of glass, aramid, carbon or other synthetic fibres impregnated with a thermoset or a thermoplastic resin. For the use of FRP as non-ferrous reinforcement in concrete bridges these materials possess several assets due to material properties such as high tensile strength, low weight and good durability characteristics. However, most FRP elements exhibit a relatively low modulus of elasticity compared to steel (Fig. 2). Furthermore, the lack of yielding involves a brittle ultimate state of FRP reinforced concrete elements.

2.1 Reinforcement materials

Two types of Glass Fibre Reinforced Plastic (GFRP), developed in the Eurocrete project, is selected for use in the trial bridge. *Plytron* bars made of E-glass and polypropylene are used as shear links. The *Eurocrete reinforcement bar (E bar)* which is a composite with higher stiffness and strength is adopted as main reinforcement. These bars are made of E-glass and vinylester matrix. For the post-tensioning of the bridge Parafil tendons were utilised. The tendons are made from a parallel arrangement of aramid fibres and are sheathed with an extruded polyethylene. At each end the filaments are anchored to conical bored end terminators by means of spikes [Fig. 6].

Material properties for the FRP materials used in the bridge are listed in Tab. 1.

	E [GPa]	f_u [MPa]	α [K^{-1}]	\emptyset [mm]	ρ [g/cm^3]
<i>Plytron</i>	23.4	520		9	1.4
<i>Eurocrete bar (E-bar)</i>	45.0	1000		13.5 / 22	2.2
<i>Parafil tendon</i>	126	1926	-7.7×10^{-5}	40	1.4

Tab. 1 Material properties

3. Design Aspects

The trial bridge was designed in accordance with the Norwegian concrete code NS 3473 [1] using supplementary provisions developed within the Eurocrete project [2]. The most relevant aspects are summarised in the following:

- A material coefficient of 3.3 is used for both types of ordinary reinforcement at ULS, while a factor of 2.0 is applied to the prestressing material. The relatively high material factors are applied to compensate for the uncertain long term effects of the FRP bars.
- Since the FRP reinforcement will not be sensible for corrosion attack, the concrete cover is reduced from a normal requirement of 50 mm to 25 mm, where the required cover is that necessary to ensure the load transfer between the concrete and reinforcement.
- Owing to the high corrosion resistance the limiting crack width is related to structural integrity and aesthetics rather than to durability. This warrants a relaxation of the normal crack width criteria from 0.2 to 0.5 mm.
- Using the basic approach for minimum reinforcement common in most codes, the strength of the concrete is replaced by an equivalent amount of reinforcement. For FRP reinforcement this amount is increased by a factor equal to the material coefficient.
- Anchorage and splicing are conservatively calculated using the bond characteristics of plain bars.
- The reduced stiffness of the longitudinal reinforcement needs to be accounted for in computing the 'concrete contribution' to the shear resistance. This effect is considered by reducing the area of longitudinal reinforcement by the factor E_{FRP}/E_{STEEL} .

4. Bridge Design

The trial bridge is erected at the Oppegård golf course located near Oslo in connection with the extension of the course from 12 to 18 holes. With a total length of 10 m the bridge is spanning over a stream separating the new laid course from the former. Apart from pedestrians the bridge accommodates a service vehicle with a total axle load of 5.5 tonne.

The main criteria for the choice of the structure were architectural quality of the bridge, its harmonisation with the site and the ambient distinctive golf course aesthetics. Additional design

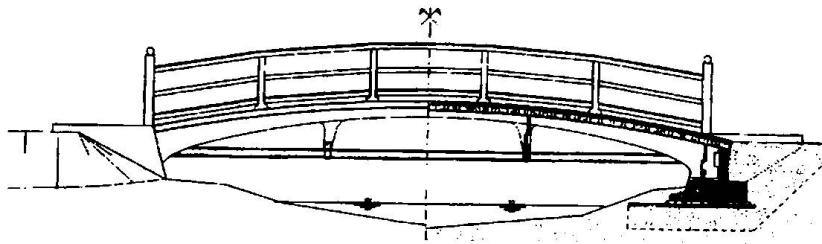


Fig. 3 Elevation and longitudinal section of the trial bridge

considerations were the requirement for prefabrication for optimum control and the intended field testing. Preference was given to a girder bridge with an arched shape. Owing to the low stiffness of the main GFRP bars, the application of prestressing was inevitable. To add to the innovative nature of the project it was decided to use FRP also for the tendons.

4.1 Edge girders

Two separate concrete edge girders carrying a wooden bridge deck constitute the bridge's superstructure (Fig. 3). The edge girders are independently resting on two conventionally reinforced abutments superficially founded on gravel beds. The statical system of the edge girders is that of an arc with a subtending post-tensioned concrete chord. Sagging necessitated the latter to be suspended by means of two conical concrete ties.

The curved compression chord has a rectangular cross section with a constant width of 300 mm and a depth increasing from 280 mm at mid-span to 650 mm at the supports. Three continuous E bars $\text{\O}22$ mm on each face provide the longitudinal reinforcement, whereas $\text{\O}9$ mm Plytron bars, formed as conventional double-legged steel links, were used for the stirrups. The formability of these bars allowed the use of FRP also for reinforcing the suspension members.

Due to the predominant compression, only minimum reinforcement was provided in the lower chord. Four $\text{\O}13.5$ mm E bars constitute the minimum longitudinal reinforcement. As a consequence of the small dimensions of the chord measuring only 250×150 mm, the Plytron bars proved however not suitable for the intended stirrup configuration. Thus special purpose-made composite links were used. The links were manufactured by roving a rectangular profile from which the continuous links subsequently were cut.

The application of the Parafil system as internal, unbonded tendons required special anchor sleeves to be made allowing the free movement of the end terminators during post-tensioning. The encapsulating sleeves (Fig. 6) were made from two cylindrical halves which were joined around the terminators and welded prior to the installation of the cable into the formwork. Between the sleeves a PVC duct is protecting the tendon from the surrounding concrete. The tendons were tensioned to approx. 30 % of the short term nominal breaking load (90 tonne). The residual working load due to creep, shrinkage and relaxation is estimated to be approx. 22 % of NBL which necessitates the girders to be re-tensioned prior to the bridge is opened for traffic.

5. Construction

The FRP reinforcement for the compression chord were pre-assembled outside the formwork. Owing to the thermoset resin used in the Plytron bars, the stirrups can be formed correspondingly

to conventional steel stirrups using a new concurrent heat-bend-twist technique. The Eurocrete bar can not be bent in the same way, but the moderate curvatures allowed for elastic bending of the bars. Installation of the pre-assembled rebar units into the formwork followed easily by hand power due to the low weight of the FRP bars (Fig. 4).

The edge girders were monolithically casted one by one with the side face down. After demolding and still in the lying position, the girders were post-tensioned to 40 % of the initial working load and temporarily locked off. The tendons were stressed to the target stress level after to the girders had been lifted in upright position and the selfweight was activated. The edge girders (Fig. 5) were transported on a truck from the pre-casting plant to the erection site. With a crowfoot hoisting wire the 4 tonne girders were lifted onto the bearings without causing additional moments in the concrete chord.

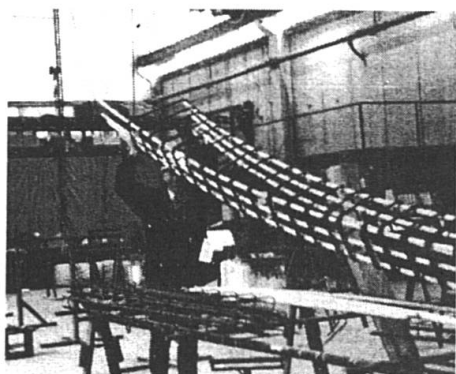


Fig. 4 Weight demonstration.



Fig. 5 Transportation of the edge girders to site

6. Instrumentation and monitoring

The documentation of the 'real-life' behaviour of the FRP reinforcement - immediate and long-term - has been of paramount interest in performing the field experiment. Measurement data from the performance monitoring provide valuable correctives to the wide range of scaled laboratory tests conducted within the Eurocrete programme. A vital link between theory and practice is further found through the comparison of the observed behaviour to the design predictions, validating the theoretical models and analytical approach employed for the response predictions.

6.1 Instrumentation

The field instrumentation is arranged for deformation and deflection monitoring, which includes measurements of concrete and reinforcement strains together with level readings. For the monitoring of concrete deformations both edge girders were equipped with internal strain gauges. The strain gauges, all of the type vibrating-wire, were located in the mid-span section of each girder, distributed in pairs to three different levels. Fig. 5 depicts the general arrangement of the instrumentation (concrete strain gauges) installed in the reference girder.

Warranting special attention is the implementation of a set of new reinforcement strain gauges especially developed for the project by *Geonor*. The reinforcement gauge is based on the

vibrating wire concept with the prestressed wire suspended between two steel muffers fixed to the bar. In both chords the longitudinal FRP reinforcement bars were equipped with the rebar transducers placed in the centre of the girder. A simple and inexpensive method was adopted for measuring the span deflections. An array of level studs cast in on top of each girder constitutes the measure points, from which level readings are taken.

As the acquisition of load performance data is ongoing, an interpretation of the 'real-life' behaviour will be presented at the conference.

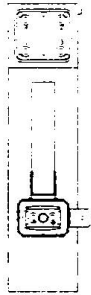


Fig. 5 Arrangement of strain gauges at midspan

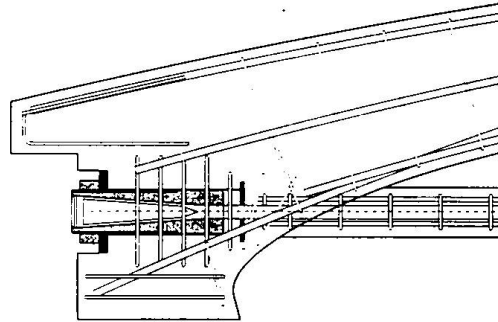


Fig. 6 Anchor zone

7. Conclusion

The erection of the Opegård trial bridge demonstrates the feasibility of the application of FRP reinforcement as supplement or even instead of steel. Owing to the inherent assets of non-ferrous composites, these materials have potentials to become prominent construction materials fighting the corrosion related deterioration of concrete structures. The vistas of a widespread use FRP is however overshadowed by the fact that there is a total shortcoming of international standards for testing, approval and quality control. Moreover the key advantages of FRP are so far lost in high material and manufacturing costs. There are however, several ongoing R & D projects continuously working to form a basis for future codes and regulations that will handle provisions for the use of FRP as a reinforcing material. Furthermore, material and manufacturing cost will decrease with a higher demand. For increased flexibility in design and construction special attention should be devoted the development of efficient mechanical applications, such as connectors, end anchorages etc.

References

- [1] Norwegian Standard NS 3473 E: Concrete structures, Design rules. 4th edition , Nov. 1992.
- [2] Clark, J. L., O'Reagen, D. P., Thirugnanendran, C.: Modification of Design Rules to Incorporate Non-ferrous Reinforcement. Eurocrete Report, January 1996.

Potsdamer Platz: Steel Fibre Concrete for Underwater Concrete Slabs

Horst FALKNER
 Prof. Dr.-Ing.
 TU Braunschweig
 Braunschweig, Germany

Horst Falkner, born 1939, received his civil engineering degree in 1964, his PhD in 1969 and became professor for concrete design in 1988.

Volker HENKE
 Dr.-Ing.
 TU Braunschweig
 Braunschweig, Germany

Volker Henke, born 1947, received his civil engineering degree in 1973, his PhD in 1980 and is a senior member of the same institute.

Summary

For the erection of a new multifunctional town centre in the heart of Berlin, in the area of Potsdamer Platz, the construction of deep building pits becomes necessary. As, due to environmental protection requirements, sealing injection layers can not be carried out for the deeper parts of these building pits, back anchored underwater slabs have to be constructed. In order to increase the overall safety of these slabs, steel fibre instead of plain concrete was used. This paper gives a short description of the tests carried out concerning the load carrying and deformation behaviour and of the site tests carried out for the erection of these slabs.

1. General

One of the first major construction measures in Berlin after the reunification is the development of the „Potsdamer Platz“ by Daimler Benz. In the former border area between the western and eastern part of the city, this building project has total dimensions of 560 m length and between 100 and 270 m width.

This building project, with foundation depths between 9 and 18 m, has to be founded in the ground-water, which has a level approximately 2 to 3 m below the surface. At the same time a connection between this building project and a new regional railway station is planned. This station has a foundation depth of up to 21 m, resulting in a water maximum pressure on the foundation slab of 180 kN/m².

Not only the building project discussed here, but all other building projects in the „Central Region“ of Berlin have to be erected in the ground-water. It has to be mentioned here, that Berlin gets its drinking water from this ground-water reservoir and therefore any encroachment into the fragile ground-water balance has to be avoided. For this reason any ground-water lowering must, on principle be excluded. In general, the following construction principles for the erection of deep building pits can be used (Fig. 1).

- The building pit walls reach into a deep, naturally sealing soil layer.
- Building pit walls in connection with a deep-laying injected soil layer which has to be arranged in such a depth that the dead soil weight compensates the water pressure with sufficient safety.
- Building pit walls in connection with an underwater concrete slab, anchored against the water pressure with tension piles in the underlying soil (wall/slab system).

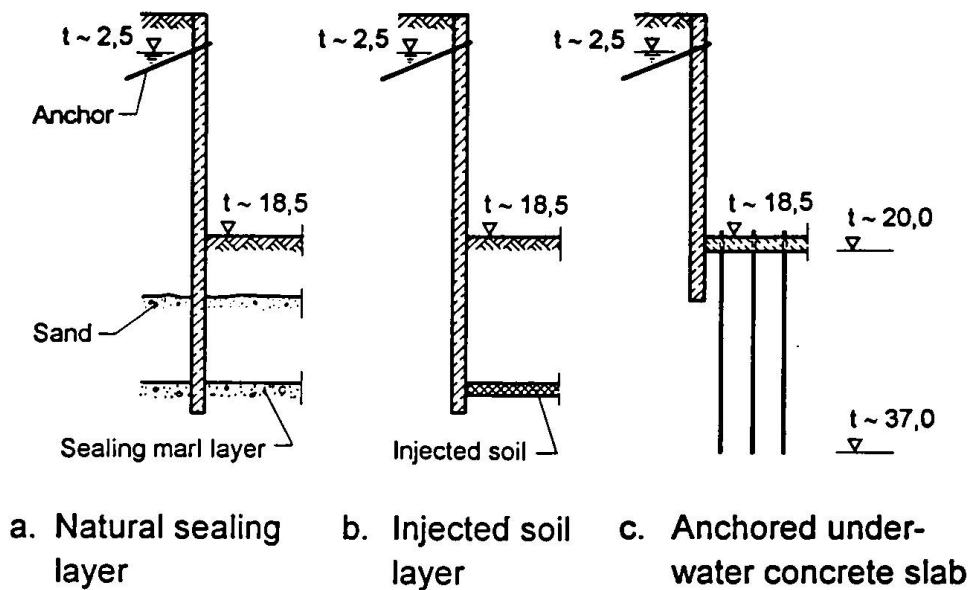


Fig. 1: Construction principles for deep building pits

The first two construction methods presented here, can, as the geological preconditions are not fulfilled, normally not be carried out. Furthermore, the deep building pit walls would interfere considerably with the ground-water flow. Therefore, this construction method can only be applied for those parts of the building pit with a depth of up to 14 m. The advantage of this method is that the excavation can be carried out in a dry building pit.

For greater depths only the so called wall/slab system can be used. This paper deals with new technologies and developments applied in the construction of the deepest parts of the building pits, where steel-fibre concrete was used on a large scale for the first time.

2. Wall/Slab System

According to Fig. 2c the construction of the building pit comprises the following steps.

- Driving of the sheet piling or construction of the slotted walls
- Excavation of the building pit to the ground water level and setting of the anchors
- Further underwater excavation down to the required level
- Driving of the tension piles from a pontoon, in this case steel profiles as vibration injected piles
- Concreting of the underwater concrete slab
- Pumping out of the building pit, after hardening of the underwater concrete slab
- If necessary, local defects have to be sealed by injections

The task of this underwater concrete slab, in connection with the tension piles, is to secure the overall stability as well as the water tightness of the building pit.

3. Steel Fibre Reinforced Concret Slabs

Normally the verification of such an underwater concrete slab is based on a simple computational model. It is assumed, that the external loading is carried by spatial arches within the slab towards the anchoring points of the tension piles, whereas the resulting horizontal force is balanced by the

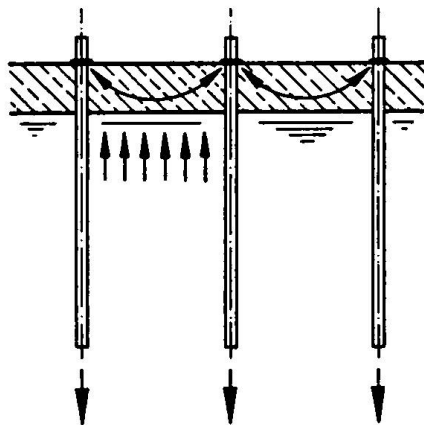


Fig. 2: Simple computational model for the verification of underwater slabs

external earth and water pressure on the surrounding walls. These anchoring points are normally considered to be fixed (Fig. 2).

Such a simple computational model is under normal circumstances sufficient for the successful erection of underwater slabs in smaller, straight building pits. For large area building pits with irregular shapes and misalignments within the slab, it has to be assumed and was shown by calculations that bending moments within the slab due, to a different load deformation behaviour of 2,000 piles, water pressure and the external normal force are unavoidable. Therefore, it was intended to avoid the brittle behaviour of a plain concrete slab and to obtain a robust and ductile construction, using steel fibre concrete.

3.1 Tests on Plain and Steel Fibre Reinforced Concrete Slabs

In order to carry out additional laboratory tests on larger scale test specimens, funds were made available by the client in order to examine the load carrying and deformation behaviour of these slabs. These tests were carried out at the iBMB laboratory on one plain and two steel fibre reinforced slabs with dimensions of 3 • 3 m and a thickness of 28 cm. One important feature of these tests, the simulation of an evenly distributed high water pressure was realized with the simple but reliable concept of a layer of cork plates underneath the test specimen. The load was applied by 9 hydraulic jacks as indicated in Fig. 3. For the first fibre reinforced slab the fibre content was 60 kg/m³ DRAMIX 60/0.8 and for the second 40 kg/m³ DRAMIX 50/0.6.

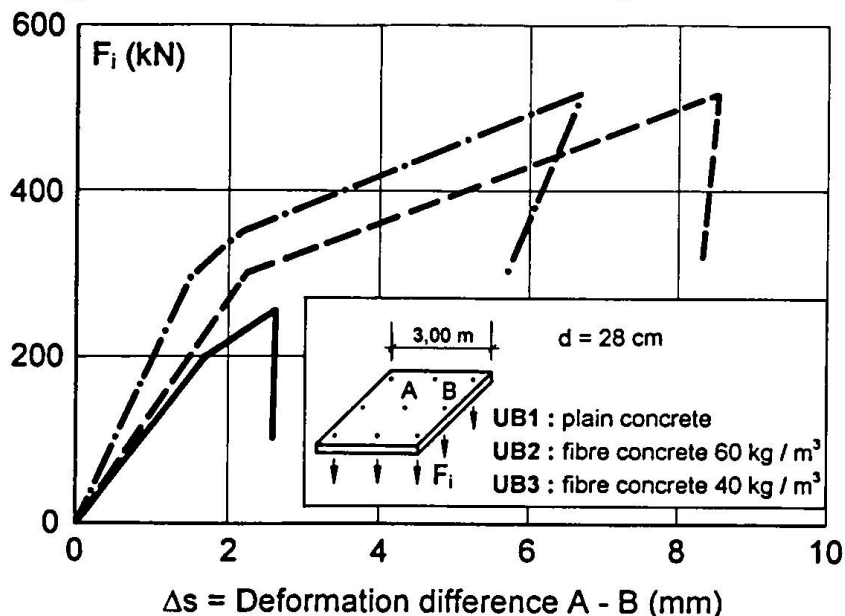


Fig. 3: Results of test loading - plates with plain and steel fibre concrete

The test results (Fig. 3) can be summarized as follows. The ultimate load bearing capacity of the plain concrete slab was reached by exceeding the concrete tensile strength. At this point, an

unannounced and sudden brittle failure occurred, the slab broke up into several pieces (Fig. 4). In comparison to this failure mode, the fibre reinforced slabs showed an entirely different behaviour. It can be seen from Fig. 3 that in comparison to the plain concrete slab, the ultimate load bearing capacity of the steel fibre reinforced slabs was more than doubled.

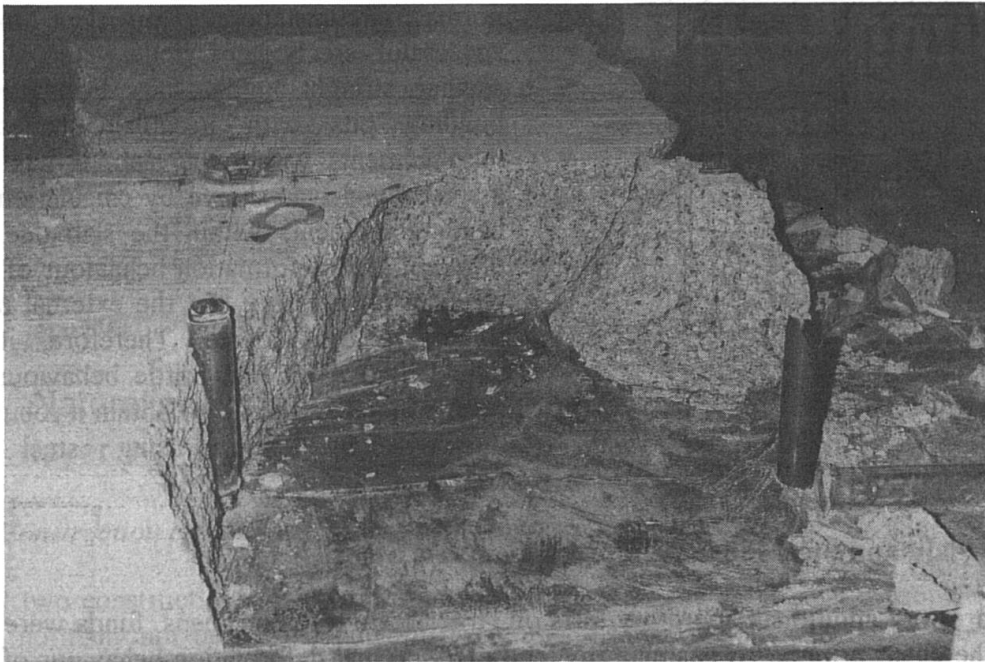


Fig. 4: Remains of the plain concrete slabs after failure

One other important aspect is the high deformability of the steel fibre reinforced slabs. It can be seen from Fig. 3 that the deformation of these slabs reached during the test is 3 to 4 times larger compared to those of the plain concrete slab. This means that steel fibre reinforced concrete slabs show an extremely ductile deformation behaviour which - as different deformations due to ground movements in such a large building pit can not be excluded - will add to the overall safety and reduces or even excludes the risk of a sudden failure.

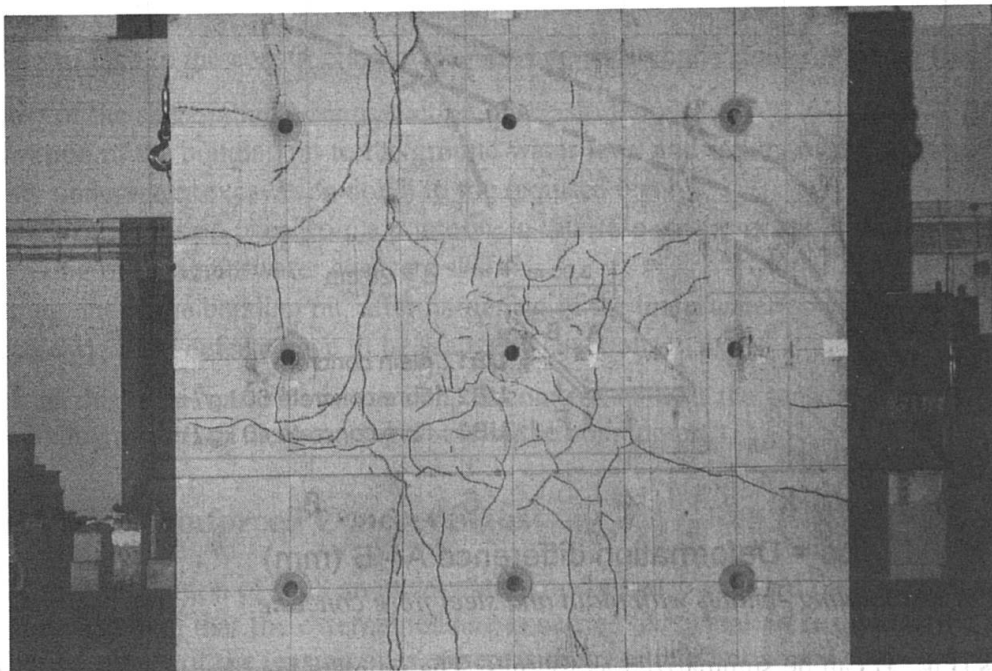


Fig. 5: Specimen with steel fibre content of 40 kg/m³ concrete

These results showed clearly, that steel fibre reinforced concrete slabs have an inherent additional redundancy and therefore possess a higher degree of performance safety. The fibre reinforced slabs did not break into several pieces, in contrary, they could be lifted as a whole from the test floor. One of the fibre reinforced test slabs can be seen in Fig. 5, where the yield lines are clearly recognizable. From this yield line pattern a simple model was developed for the dimensioning of these slabs.

4. Large Scale Tests on the Building Site

Under German building regulations, building materials which are not covered by normal building standards and/or codes have to obtain a special permission. This ensures that the new building material or method conforms with existing standards. In this context, it had to be proven in a large scale test under building site conditions that the following conditions could be met:

- Pumping of steel fibre concrete over long distances
- Concrete hardening and compacting under water
- Aggregate and fibre distribution over the cross-section
- Enclosure of the pile-heads
- Low heat of hydration.

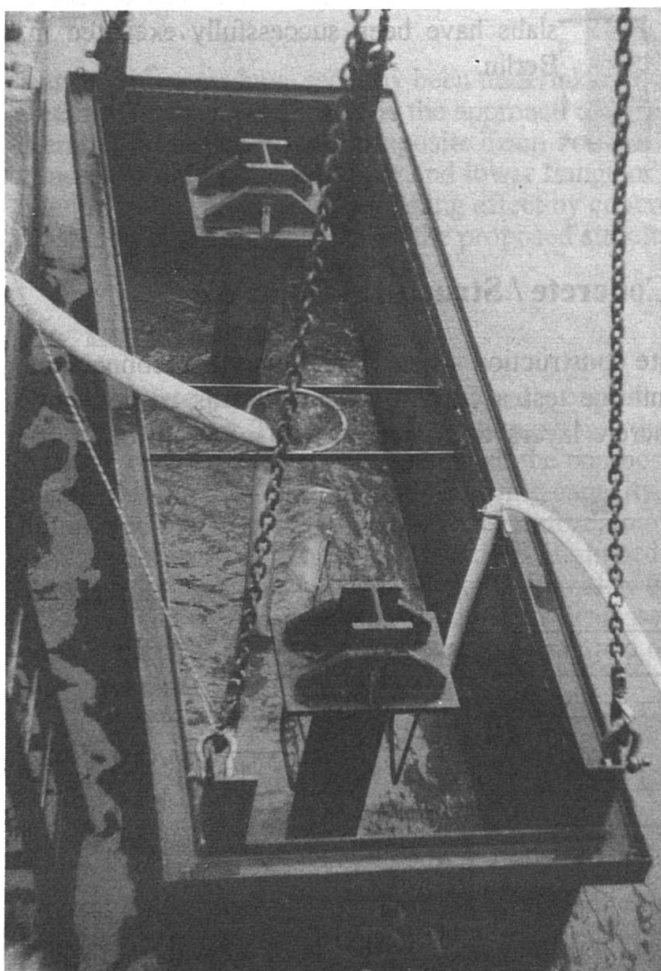


Fig. 6: Steel container with two pile heads

These additional tests were carried out by a test concreting with different concrete mixes into steel containers. Fig. 6 shows the steel container of one test specimen prior to lowering into the building pit. The cross-section of these containers was 1.2 • 1.2 m with a total length of 4.0 m.

A total of 6 underwater concreting tests, together with 4 additional pumping tests, had to be carried out. The six underwater concreting tests were necessary as - even though the concrete mixes were based on extensive preliminary laboratory tests with regard to the concrete properties, composition and slump - some of the first mixes showed an extremely high retarding time. Even if these concretes reached their intended strength (C 20/25) in the end, such an unpredictable behaviour could not be tolerated. Therefore, these tests proved to be really valuable, as they showed the behaviour of the different concrete mixes under building site conditions in comparison to defined laboratory conditions. In order to prove, that the heads of the tension piles were totally enclosed by the steel fibre concrete and, additionally, that there was an even steel fibre distribution over the cross

section, the test specimen had to be cut through the pile head.

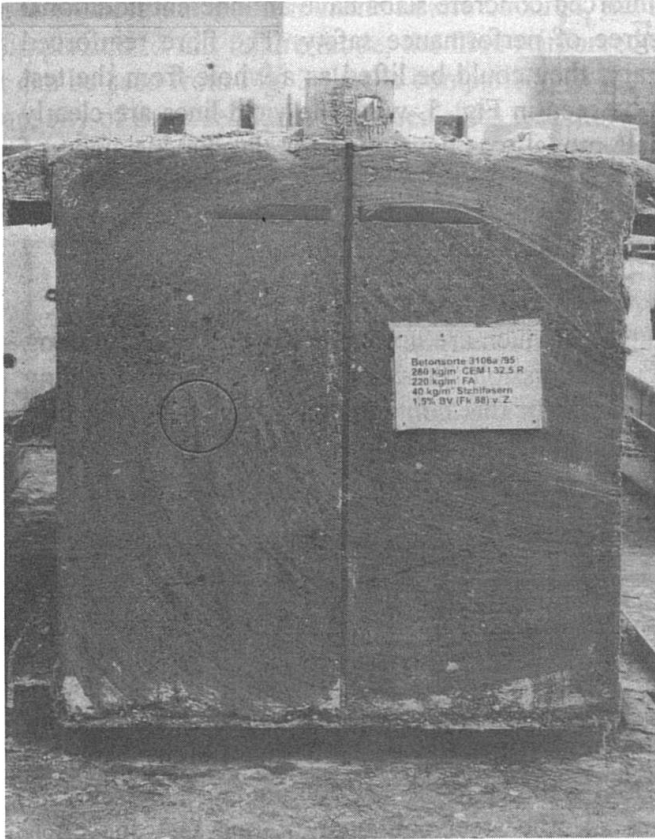


Fig. 7: Cross-section of a test specimen

Fig. 7 shows the cross section through such a test specimen which was cut with a diamond saw. The close inspection showed, that the pile head was properly enclosed by the steel fibre concrete, an even fibre distribution over the cross section can be achieved and no disintegration of the concrete structure did occur.

The laboratory tests and the concreting tests on the building site showed that all required preconditions set for the special approval could be met. Therefore, it was finally decided to use this new technology for the deep building pits at the Potsdamer Platz.

In the meantime more than 40,000 m² of underwater steel fibre reinforced concrete slabs have been successfully executed in Berlin.

5. Composite Behaviour - Steel Fibre Concrete / Structural Concrete

In order to examine the behaviour of a composite construction - steel fibre concrete in connection with the overlaying structural concrete - a tentative test according to Fig. 8 was carried out. During the test the joint between the two concrete layers was injected with water in order to simulate the later water pressure.

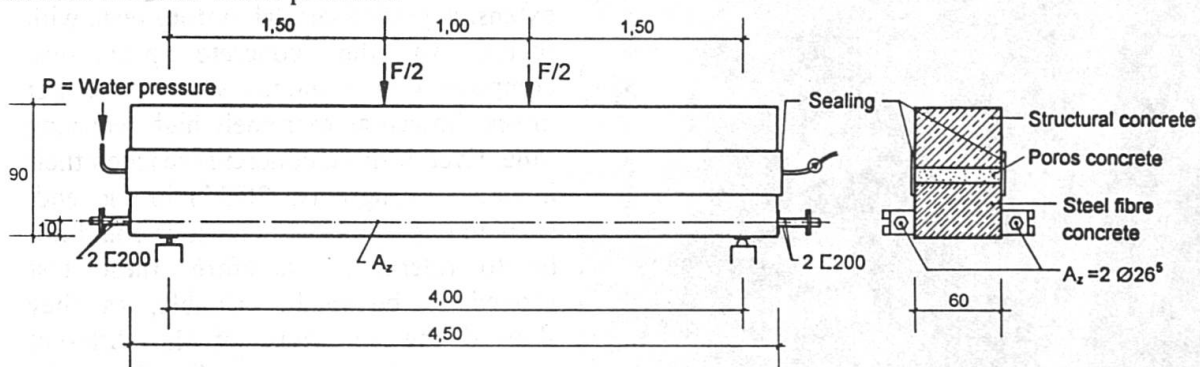


Fig. 8: Composite beam test set-up

The test results can not be discussed here in detail, but they showed that both parts of the beam act more or less monolithically together and that the ultimate load of such composite construction is close to that of a monolithical beam. This means, that the consideration of such a composite behaviour in the actual design would lead to a more economical construction due to a reduction in the overall thickness and a reduction in excavation work.